LBL-38645
UC-414
Preprint

Lawrence Berkeley Laboratory
UNIVERSITY OF CALIFORNIA

Physics Division

Submitted to Nuclear Physics B

The Inverse Amplitude Method in Chiral Perturbation Theory

A. Dobado and J.R. Peláez

April 1996

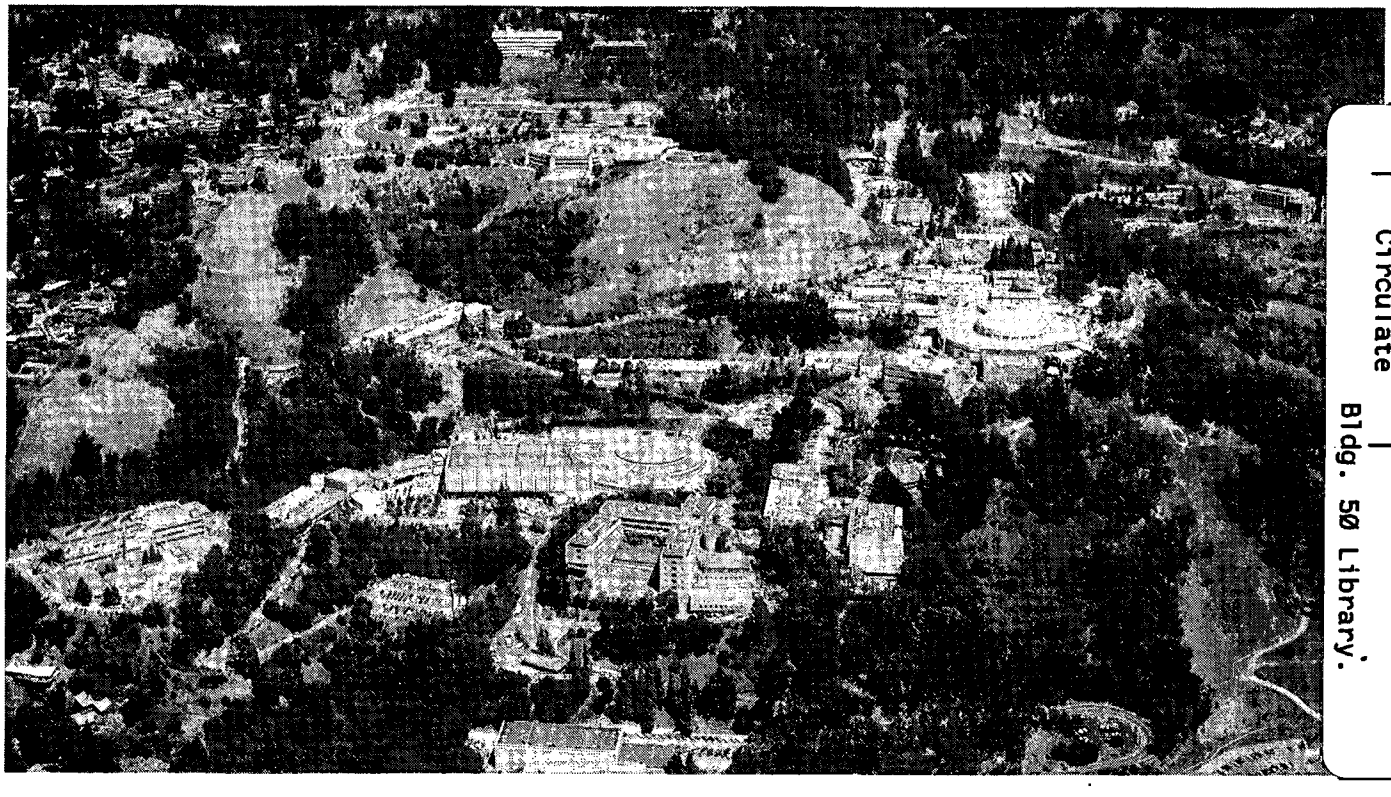

REFERENCE COPY
Does Not
Circulate
Bldg. 50 Library.
LBL-38645
Copy 1

Prepared for the U.S. Department of Energy under Contract Number DE-AC03-76SF00098

DISCLAIMER

This document was prepared as an account of work sponsored by the United States Government. While this document is believed to contain correct information, neither the United States Government nor any agency thereof, nor the Regents of the University of California, nor any of their employees, makes any warranty, express or implied, or assumes any legal responsibility for the accuracy, completeness, or usefulness of any information, apparatus, product, or process disclosed, or represents that its use would not infringe privately owned rights. Reference herein to any specific commercial product, process, or service by its trade name, trademark, manufacturer, or otherwise, does not necessarily constitute or imply its endorsement, recommendation, or favoring by the United States Government or any agency thereof, or the Regents of the University of California. The views and opinions of authors expressed herein do not necessarily state or reflect those of the United States Government or any agency thereof or the Regents of the University of California.

LBL-38645
UCM-FT 3/96
April 1996

The inverse amplitude method in Chiral Perturbation Theory [1]

A. Dobado[2]
Departamento de Física Teórica.
Universidad Complutense. 28040 Madrid, SPAIN
and
J.R. Peláez[3]
Theoretical Physics Group. Lawrence Berkeley Laboratory
University of California. Berkeley, California 94720. USA.

Abstract

Based on a dispersive approach, we apply the inverse amplitude method to unitarize the one-loop $SU(2)$ and $SU(3)$ Chiral Perturbation Theory. We find that this unitarization technique yields the correct complex analytical structure in terms of cuts and poles. As a matter of fact, we obtain the poles associated to the $\rho(770)$ and $K^*(982)$ resonances. We obtain their masses and widths within a 15% error, when using the present chiral parameter estimates obtained from low energy experiments. However, by fixing the actual mass values of both resonances we obtain a parametrization of the $\pi\pi$ and πK phase shifts up to the first inelastic threshold, which yields the correct values of their widths. With this fit we have also calculated several phenomenological parameters, including the scattering lengths, which can be of interest for future experiments.

[1]This work was supported by the Director, Office of Energy Research, Office of High Energy and Nuclear Physics, Division of High Energy Physics of the U.S. Department of Energy under Contract DE-AC03-76SF00098.

[2]e-mail:dobado@cernvm.cern.ch

[3]Complutense del Amo fellow. On leave of absence from: Departamento de Física Teórica. Universidad Complutense. 28040 Madrid,SPAIN. e-mail:pelaez@theorm.lbl.gov, pelaez@vxcern.cern.ch

1 Introduction

Even though QCD has been repeatedly confronted with experiments and it yields a remarkably good description of the strong interaction, the low energy hadron physics has to be modelled phenomenologically. This is due to the fact that the usual perturbative approach in the coupling constant cannot be applied to QCD below energies of the order of 1 GeV. Most of the phenomenological results were based on PCAC and the so called Current Algebra. However, in 1979, Weinberg [1] showed how to reobtain many of these predictions by means of an effective lagrangian.

The fields in such a lagrangian are the light mesons, (pions, kaons and etas) which are understood as the Goldstone Bosons (GB) arising from the spontaneous breaking of chiral symmetry. Such a lagrangian should be built as an expansion in derivatives, but respecting the symmetry patterns of QCD, namely, the chiral symmetry breaking. Indeed, the first term in the expansion is fixed by the symmetry requirements and accounts for the Current Algebra results. The main advantage of this procedure is that the next terms in the expansion produce further corrections, which depend on several phenomenological parameters but are always consistent with the QCD symmetry constraints. More than ten years ago, these techniques were developed to the one-loop level in a set of papers by Gasser and Leutwyler [2, 3], where they showed how to derive Green functions involving light mesons, as functions of their momenta, their masses and those few phenomenological parameters.

By fitting these parameters from a small number of low energy experiments it is then possible to obtain succesfull predictions for many other processes. A great deal of papers have appeared in the literature following this approach which is known as Chiral Perturbation Theory (ChPT).

While we were preparing this work some partial higher order calculations [4] have appeared in the literature as well as a complete two loop calculation of $\pi\pi$ scattering [5], which will be needed in order to analyse new and more precise data to come from DAΦNE and Brookhaven. For a general review of the present status of experimental data on pion physics and future prospects, we refer the reader to [6].

Nevertheless, there are some intrinsic limitations when applying ChPT, namely, the fact that the amplitudes calculated within the chiral approach are only unitary in the perturbative sense. That is, up to the next order in external momenta. Such a breakdown of unitarity is most severe at high energies, consistently with the approximation, although it can also occur at moderate energies [7]. As a result, it is not possible to reproduce resonant states, which are one of the most characteristic features of the strongly interacting regime. Many different methods have been proposed in order to improve this behavior and thus to extend the applicability of ChPT to higher energies; among them: The use of Padé approximants [8], the explicit introduction of resonances [9, 10], the large N limit [11] (N being the number of GB) or the inverse amplitude method (IAM) [7, 8, 12, 13].

This work is devoted precisely to the last method, which can be justified within a dispersive approach, and it has been shown that it can easily reproduce the two lowest resonances: the $\rho(770)$ resonance in $\pi\pi$ scattering [8] and the $K^*(892)$ resonance in πK scattering [12].

But not only that, the IAM is also able to improve considerably the fit to experimental data even in those channels where there are no resonances. This fit provides a remarkably good parametrization up to high energies, that can be used for other processes. Indeed, in a previous work [14], the authors showed how it can be used together with a simple unitarization prescription to obtain succesful results on $\gamma\gamma \to \pi^0\pi^0$ up to 700 MeV.

Of course, it is also possible to obtain very good parametrizations [9, 10] of $\pi\pi$ or πK elastic scattering up to very high energies, by including all resonant explicitly, which can be very useful for further analysis. However, our aim with the IAM is to be able to reproduce this phenomena just with the few phenomenological parameters present in the ChPT lagrangian. In this way, the resonances can be regarded as real predictions of the model.

The purpose of this work is to study how high in energies the IAM can still yield good results and what are its limitations. In view of its remarkable success, fitting resonances at energies as high as 890 MeV, we would also like to know whether it is possible to reproduce further resonance states. It is clear that the best candidates are the lightest resonances whose dominat decay modes are $\pi\pi$ or πK. We have listed them in Table 1, where we can see that some of them, as the $f_0(980)$, are not much heavier than other resonances that the IAM reproduces amazingly well. In case these resonances were not accomodated after our unitarization, it would be interesting to understand why.

Name	I,J	Mass	Width	Dominant decays
$\rho(770)$	1,1	768.8 ± 1.0	150.3 ± 1.0	$\pi\pi$, 100%
$f_0(980)$	0,0	980 ± 10	40 to 400	$\pi\pi$, $(78.1 \pm 2.4)\%$ $K\bar{K}$, $(21.9 \pm 2.4)\%$
$f_2(1270)$	0,2	1275 ± 5	185 ± 20	$\pi\pi$, $(84.7 \pm 2.6)\%$
$K^*(892)^\pm$ $K^*(892)^0$	1/2,1 1/2,1	891.59 ± 0.24 896.10 ± 0.28	49.8 ± 0.8 50.5 ± 0.6	πK, $\simeq 100\%$

Table 1: Lightest resonances with $\pi\pi$ or πK dominant decay modes. Data taken from [15].

Finally, we would like to comment another motivation of the present work, which at first may not seem very related with the main topic. The philosophy of the chiral approach has also reached other fields of particle physics. That is the case of the strongly interacting symmetry breaking sector (SISBS) of the Standard Model [16]. The scalar sector of such a model displays the same symmetry breaking pattern as a two flavor massless QCD. It is then possible to build an effective lagrangian, for the electroweak Goldstone Bosons, much as we commented before for QCD [17]. In this case the GB are not physical, but using this lagrangian it is possible to obtain predictions on the scattering of longitudinal weak bosons [18] at future colliders like LHC. Indeed, there are already experimental proposals to measure the chiral parameters of the effective elctroweak parameters at CMS [19]. Most of the works on the SISBS make use of the so called Equivalence Theorem [16], which allow

us to read the observable amplitudes, in terms of longitudinal gauge bosons, directly from those with GB. This theorem has been recently proved in the chiral lagrangian formalism [20] and seems to be severely constrained by the lack of unitarity. At this point is when the unitarization procedures come into play. But now it is crucial to know whether a given unitarization prescription is applicable and reliable, since what we are now looking for are real predictions and not elaborated fits to still unavailable data.

In Section 2 we review some basic aspects of exact and perturbative unitarity and we define the partial waves in elastic scattering. Section 3 introduces the IAM, first with a derivation from Dispersion Theory and then by studying the constraints to its applicability. Section 4 and Section 5 are organized in the same way, although they refer to $SU(2)$ and $SU(3)$ ChPT, respectively. Indeed in both them we first apply the IAM to ChPT with the chiral parameters obtained from low energy experiments in order to study the IAM predictive power; next they present an IAM fit to the data. For the best $SU(3)$ fit we present the unitarized results for the scattering lengths and some other phenomenological parameters. Then, in Section 6, we study the analytic structure on the complex plane of the IAM amplitudes. In Section 7 we present the conclusions. There is also one Appendix where we give the elastic scattering formulae used in this work, as well as a discussion on perturbative unitarity.

2 Partial waves, phase shifts and unitarity.

When dealing with strong interactions, it is usual to project the amplitudes in states of definite angular momentum J and isospin I. The new amplitudes are called partial waves and they can be written as follows

$$t_{IJ}(s) = \frac{1}{32K\pi}\int_{-1}^{1} \mathrm{d}(\cos\theta) P_J(\cos\theta) T_I(s,t) \tag{1}$$

where $K = 2$ or 1 depending on whether the particles in the process are identical or not. The acceptable isospin values also depend on the process, namely $I = 1, 2, 3$ for $\pi\pi$ elastic scattering and $I = 1/2, 3/2$ for πK. For both reactions the definite isospin amplitudes T_I are obtained from a single function. In the first case:

$$\begin{aligned} T_0(s,t,u) &= 3A(s,t,u) + A(t,s,u) + A(u,t,s) \\ T_1(s,t,u) &= A(t,s,u) - A(u,t,s) \\ T_2(s,t,u) &= A(t,s,u) + A(u,t,s) \end{aligned} \tag{2}$$

whereas for πK scattering we can write:

$$T_{1/2}(s,t,u) = \frac{3}{2}T_{3/2}(u,t,s) - \frac{1}{2}T_{3/2}(s,t,u) \tag{3}$$

In order to deal with both processes on the same footing, we will label the particles in the reaction as α and β, so that, for instance, the Mandelstam variables will satisfy:

$s+t+u = 2(M_\alpha^2 + M_\beta^2)$. Hence the threshold will be at $s_{th} = (M_\alpha + M_\beta)^2$. As it is well known, whenever $s > s_{th}$, and below inelastic thresholds, the unitarity of the S-matrix implies that:

$$\mathrm{Im} t_{IJ} = \sigma_{\alpha\beta} \mid t_{IJ} \mid^2 \tag{4}$$

where $\sigma_{\alpha\beta}$ is a factor that comes from the integration over the two particle phase space. Explicitly:

$$\sigma_{\alpha\beta}(s) = \sqrt{\left(1 - \frac{(M_\alpha + M_\beta)^2}{s}\right)\left(1 - \frac{(M_\alpha - M_\beta)^2}{s}\right)} \tag{5}$$

As a consequence of Eq.4, the partial wave can be parametrized as follows:

$$t_{IJ}(s) = \frac{1}{\sigma_{\alpha\beta}(s)} e^{i\delta_{IJ}(s)} \sin \delta_{IJ}(s) \tag{6}$$

and $\delta_{IJ}(s)$ is called the IJ phase shift.

We have already mentioned that ChPT is organized as an expansion in derivatives. At the amplitude level, these derivatives transform into the meson external momenta and masses. That is, we obtain the partial waves as follows:

$$t_{IJ} = t_{IJ}^{(0)} + t_{IJ}^{(1)} + t_{IJ}^{(2)} + ... \tag{7}$$

where, for the cases we are now dealing with, $t_{IJ}^{(0)}$ is $\mathcal{O}(p^2)$, $t_{IJ}^{(1)}$ is $\mathcal{O}(p^4)$, etc...(there are also some logarithms, but they are irrelevant for the present discussion). In practice, we can only obtain the few first terms of the series above, and then it is easy to realize that our amplitude cannot satisfy exactly the unitarity constraint in Eq.4. Nevertheless, they satisfy the unitarity condition perturbatively. In other words:

$$\begin{aligned} \mathrm{Im} t_{IJ}^{(0)} &= 0 \\ \mathrm{Im} t_{IJ}^{(1)} &= \sigma_{\alpha\beta} t_{IJ}^{(0)2} \\ \mathrm{Im}(t_{IJ}^{(2)} + t_{IJ}^{(1)}) &= \sigma_{\alpha\beta}\left(t_{IJ}^{(0)2} + 2t_{IJ}^{(0)}\mathrm{Re} t_{IJ}^{(1)}\right) \simeq \sigma_{\alpha\beta} \mid t_{IJ}^{(0)} + t_{IJ}^{(1)} \mid^2 \end{aligned} \tag{8}$$

As we have alredy commented, the $\mathcal{O}(p^2)$ were given by Weinberg [1] and they correspond to the so called low energy theorems. For pion elastic scattering the calculation to one loop was carried out by Gasser and Leutwyler using an $SU(2)_L \times SU(2)_R$ invariant effective lagrangian [2], although they also extended the formalism to $SU(3)_L \times SU(3)_R$ by considerding the strange quark [3]. These calculations include the dependence on the chiral parameters (called $\bar{l}_i$ for SU(2) and L_i for SU(3)) and the physical masses M_π, M_K, M_η and decay constants F_π, F_K, F_η. The precise calculation for πK scattering can be found in [21, 22], although we have found that those formulae should be slightly modified to satisfy Eq.8. We will comment on that later. Finally we want to point out that very recently it has appeared the complete calculation of the $\mathcal{O}(p^6)$ contribution to elastic $\pi\pi$ scattering [5].

3 The Inverse Amplitude Method

3.1 Derivation from Dispersion Theory

Let us briefly review the standard derivation [7, 12] of the inverse amplitude method in ChPT. Most of this discussion will be used later in order to understand the different approximations performed at each step, how they limit the applicability of the method and whether it is possible to avoid some of them.

From very general considerations, the amplitudes obtained from a relativistic Quantum Field Theory should present a characteristic analytical structure when the real variable s is promoted to a complex variable. Indeed, the production threshold for the reaction implies the existence of a cut in the complex plane which, starting at $s = s_{th}$, extends to infinity all over the positive real axis. Then, by crossing symmetry, it can be shown that there should be another left cut along the negative axis. Therefore, we can apply Cauchy's Theorem to our complex amplitudes and obtain integral equations that are known as dispersion relations. For instance, a three times subtracted dispersion relation for an exact amplitude is nothing but:

$$t_{IJ}(s) = C_0 + C_1 s + C_2 s^2 + \frac{s^3}{\pi}\int_{(M_\alpha+M_\beta)^2}^{\infty} \frac{\mathrm{Im} t_{IJ}(s')ds'}{s'^3(s'-s-i\epsilon)} + LC(t_{IJ}) \tag{9}$$

Where we have not written explicitly the left cut (LC) contribution. The minimum number of subtractions needed depends on how the amplitude behaves at infinity in order to ensure the vanishing of the contributions coming from closing the integral contour. In our example we have chosen three subtractions since we are mainly going to use $\mathcal{O}(p^4)$ ChPT amplitudes which at high s behave as s^2. But our arguments remain valid for $\mathcal{O}(p^6)$ amplitudes when using four times subtracted dispersion relations, etc...

As it should be, the partial waves obtained from ChPT do present both cuts. Indeed the chiral formalism allows us to calculate both the subtraction constants C_0, C_1, C_2 and the integrand inside Eq.9. Following with our notation we have:

$$\begin{aligned} t_{IJ}^{(0)} &= a_0 + a_1 s \\ t_{IJ}^{(1)} &= b_0 + b_1 s + b_2 s^2 + \frac{s^3}{\pi}\int_{(M_\alpha+M_\beta)^2}^{\infty} \frac{\mathrm{Im} t_{IJ}^{(1)}(s')ds'}{s'^3(s'-s-i\epsilon)} + LC(t_{IJ}^{(1)}) \end{aligned} \tag{10}$$

Where we have expanded the subtraction constants in terms of M_α^2/F_β^2.

The IAM is based on the fact that the function $1/t_{IJ}$ displays the very same analytic structure of t_{IJ}, apart from some possible pole contributions. For later convenience, we will make use of $G(s) = t_{IJ}^{(0)2}/t_{IJ}$, which is nothing but the inverse amplitude multiplied by a real number; thus we are keeping its analytic properties and we can write a very similar dispersion relation:

$$G(s) = G_0 + G_1 s + G_2 s^2 + \frac{s^3}{\pi}\int_{(M_\alpha+M_\beta)^2}^{\infty} \frac{\mathrm{Im} G(s')ds'}{s'^3(s'-s-i\epsilon)} + LC(G) + PC \tag{11}$$

where PC stands for possible pole contributions. The advantage of using $G(s)$ is that, by means of Eqs.4 and 8, we can calculate exactly the integral over the right cut, since then:

$$\mathrm{Im}G = -t_{IJ}^{(0)2}\frac{\mathrm{Im}t_{IJ}}{\mid t_{IJ}\mid^2} = -t_{IJ}^{(0)2}\sigma = -\mathrm{Im}t_{IJ}^{(1)} \tag{12}$$

Note that we are always denoting by t_{IJ} the exact amplitude, which is unknown, although we know its analytic properties. In contrast, the expressions for $t_{IJ}^{(0)}$ and $t_{IJ}^{(1)}$, etc... have been calculated explicitly.

As we did before, we can also expand the G_i subtraction coefficients in powers of M_α^2/F_β^2, and then rewrite the subtraction relation for $G(s)$, which now reads as follows:

$$\begin{aligned}\frac{t_{IJ}^{(0)2}}{t_{IJ}} &\simeq a_0 + a_1 s - b_0 - b_1 s - b_2 s^2 \\ &- \frac{s^3}{\pi}\int_{(M_\alpha+M_\beta)^2}^{\infty}\frac{\mathrm{Im}t_{IJ}^{(1)}(s')ds'}{s'^3(s'-s-i\epsilon)} - LC(t_{IJ}^{(1)}) + PC\end{aligned} \tag{13}$$

where we have approximated $\mathrm{Im}G \simeq -\mathrm{Im}t_{IJ}^{(1)}$ on the left cut. But, neglecting the pole contribution, and comparing with Eq.10, what we have just found is nothing but:

$$\frac{t_{IJ}^{(0)2}}{t_{IJ}} \simeq t_{IJ}^{(0)} - t_{IJ}^{(1)} \tag{14}$$

or, in other words,

$$t_{IJ} \simeq \frac{t_{IJ}^{(0)2}}{t_{IJ}^{(0)} - t_{IJ}^{(1)}} \tag{15}$$

Which is the well known IAM result, that we are going to use throughout the present work. Incidentally, Eq.15 can be written as the formal $[1,1]$ Padé approximant of the perturbative ChPT amplitude.

3.2 The applicability of the Inverse Amplitude Method

Let us go again through all the approximations that we have made in the previous section, in order to comment how they will constraint its applicability:

3.2.1 The left cut

We have already pointed out that in Eq.13 we have replaced the $G(s)$ left cut integral by that of $-t_{IJ}^{(1)}(s)$. As we have shown in the preceeding discussion (Eq.12), that is only valid over the right cut. Indeed, on the left cut we cannot write the chain of equalities that we have written in Eq.12. Nevertheless, we still can use the ChPT result as an approximation:

$$\mathrm{Im}G = -t_{IJ}^{(0)2}\frac{\mathrm{Im}t_{IJ}}{\mid t_{IJ}\mid^2} \simeq -\mathrm{Im}t_{IJ}^{(1)} + \mathcal{O}(p^6) \tag{16}$$

And thus we get

$$LC(G) = \int_{-\infty}^{0} \frac{\mathrm{Im}G_{IJ}(s')ds'}{s'^3(s'-s-i\epsilon)} \simeq -\int_{-\infty}^{0} \frac{\mathrm{Im}t_{IJ}^{(1)}(s')ds'}{s'^3(s'-s-i\epsilon)} = -LC(t_{IJ}^{(1)}) \tag{17}$$

Notice that, in order to obtain the IJ phase shifts, we are going to calculate $t_{IJ}(s)$ for real $s > 4M_\pi$. That means that the denominator $(s'-s-i\epsilon)$ inside the integrals is never going to be very small, which somehow will wash out the error we make when we approximate ImG. Nevertheless, with the inverse amplitude method we will not get the same function of the logarithms in u and t that we obtain with plain ChPT. We expect this effect to be rather small since the logarithms are dominated by power like contributions.

3.2.2 The pole contribution

When passing from Eq.13 to Eq.14, we have neglected the contributions coming from zeros in the amplitude, that will appear as poles of the inverse function. There is no way to know *a priori* whether or not a partial wave will vanish for some s value and in practice we can only guess their existence by inspection of our results. Nevertheless, in case they existed, their contribution can be taken into account with a subtraction in these points. As far as from our results we have never found any hint of such a pole, we have not developed further this possibility.

3.2.3 Multiplying by $t_{IJ}^{(0)}$

This is apparently the harmless assumption in the reasoning above, although it dramatically affects the results of the IAM. In fact, it can happen that $t_{IJ}^{(0)} = 0$. This is not the case for the $(I,J) = (0,0),(1,1),(2,0)$ channels in $\pi\pi$ scattering nor for $(3/2,0),(1/2,0),(1/2,1)$ for πK. However, any other partial wave vanishes at $\mathcal{O}(p^2)$. That means that our formula in Eq.15 is no longer valid.

Nevertheless, we can try to generalize our previous derivation of the method, in order to include those channels whose leading order is given by $\mathcal{O}(p^4)$. It is indeed possible, and we only have to go through the very same steps, although now we would write a dispersion relation for $t_{IJ}^{(2)}$. But let us remember that the main improvement of the approach is that we are calculating exactly the integral of Im$G(s)$ over the right cut. However, for that purpose we obviously need some imaginary part, and by looking at Eq.8 we can see that $t_{IJ}^{(0)} = 0$ implies that $\mathrm{Im}t_{IJ}^{(1)} = \mathrm{Im}t_{IJ}^{(2)} = 0$. Therefore, unless we have a calculation up to $\mathcal{O}(p^8)$, the corresponding imaginary part will vanish. Therefore when following the derivation of the IAM if $t_{IJ}^{(0)} = 0$ the best we can get is plain ChPT again. As we have already commented, just very recently it has appeared an $\mathcal{O}(p^6)$ calculation of $\pi\pi$ scattering [4, 5]. Therefore, at present we can only expect to obtain a real improvement with our approach in the six channels listed above. In particular, the IAM in the $(0,2)$ channel yields again the ChPT result. With the present status of ChPT calculations we cannot even think about trying to reproduce the $f_2(1200)$ resonance. But that could change in the future.

3.2.4 Elastic unitarity

In order to obtain ImG in the right cut, Eq.12, we have made another approximation, which is to use of the elastic unitarity condition of Eq.4. As a matter of fact, the right cut is indeed composed of many superimposed cuts, each one corresponding to a different inelastic intermediate channel. As a consecuence, Eq.4 is only true below the first inelastic threshold, and the real unitarity condition for a generic partial wave t would read:

$$\mathrm{Im}t_{\alpha\beta\to\alpha\beta} = \sum_A \sigma_A \mid t_{\alpha\beta\to A} \mid^2 \Theta(s - s_A) \tag{18}$$

where the sum is over all the physically accesible intermediate states that we have called A. The σ_A factor is precisely the phase space corresponding to the that state A. Therefore $\Theta = 1$ whenever s is bigger than the A threshold (denoted s_A), otherwise $\Theta = 0$ (Note that some authors absorb the Θ function on the phase space factor, but we have preferred to make it explicit).

As far as we are neglecting electromagnetic interactions, the first inelastic channel in $\pi\pi$ is the four pion intermediate state, which opens at 550 MeV. Similarly, for πK is $\pi K\pi\pi$, whose threshold is $\simeq$ 910 MeV. Strictly speaking, only for energies below these values, the elastic approximation that we have used is exact. Within ChPT these processes are $\mathcal{O}(p^6)$, which would allow us to neglect them against the $\mathcal{O}(p^4)$ contributions at low energies. One of our motivations, however, is to study the IAM at high energies (of the order of 1 GeV) and therefore in that regime such a reasoning does no longer hold. Nevertheless, the contribution of these intermediate states is also supressed by the four particle phase space in Eq.18, so that we still expect the IAM to provide us with a good approximation.

There will also be other inelastic channels with more pions, opening at higher energies, but they will be even more supressed in the chiral expansion and by phase space.

Unfortunately, there are intermediate channels, within the energies that we are interested in, which are not supressed neither by the chiral counting nor by a many body phase space. Indeed, at an energy of approximately 985 MeV, the inelastic KK threshold opens up. Unfortunately, the process $\pi\pi \to KK$ has a non vanishing $\mathcal{O}(p^2)$ contribution and its phase space factor in Eq.18 is the $\sigma_{\alpha\beta}$ that we have already met in Eq.5, although with $M_\alpha = M_\beta = M_K$. Therefore, for energies above the two kaon threshold we have to reconsider the derivation of the IAM. Let us illustrate with $\pi\pi$ scattering how inelastic effects affect our result.

As the starting point, for $s > s_{K\bar{K}}$, we have a new unitarity relation:

$$\mathrm{Im}t = \sigma_{\pi\pi} \mid t \mid^2 + \sigma_{K\bar{K}} \mid t_K \mid^2 \tag{19}$$

where we have denoted by t the generic t_{IJ} pion elastic scattering amplitude and by t_K the IJ partial wave of the process $\pi\pi \to K\bar{K}$.

Once again we introduce the auxiliary function $G = t^{(0)2}/t$, whose imaginary part, always for $s > s_{K\bar{K}}$, is now

$$\mathrm{Im}G = -t_{IJ}^{(0)2} \frac{\mathrm{Im}t_{IJ}}{\mid t_{IJ} \mid^2} = -t_{IJ}^{(0)2} \left(\sigma_{\pi\pi} + \sigma_{K\bar{K}} \frac{\mid t_K \mid^2}{\mid t \mid^2} \right) \tag{20}$$

The above equation differs from Eq.12, in the term coming from two kaon intermediate production, that we will also have to take into account when computing the integral over the right cut. In contrast, on the left cut we will again approximate $\mathrm{Im}G \simeq -\mathrm{Im}t^{(1)}$, much as we did in the elastic regime.

Following the very same steps of our previous derivation, we arrive to

$$\frac{t^{(0)2}}{t_{IJ}} \simeq t^{(0)} - t^{(1)} - \frac{s^3}{\pi}\int_{4M_\pi^2}^{\infty} \frac{\sigma_{K\bar{K}}}{s'^3(s'-s-i\epsilon)} \underbrace{\left(t^{(0)2}(s')\frac{\mid t_K(s')\mid^2}{\mid t(s')\mid^2} - t_K^{(0)2}(s')\right)}_{\Delta(s')} ds' \tag{21}$$

In the above equation there are terms that we cannot calculate, as for instance, the exact t_K amplitude. Nevertheless, we could try to approximate the integrand using ChPT. In that case, we find that $\Delta(s') \simeq 0 + \mathcal{O}(p^6)$, so that one is tempted to neglect the whole integral. Apparently, it will be the same approximation that we used in the left cut. However, the actual values of s that we use in our calculations are such that the denominator can amplify the error in our approximation (notice that, if it was it not for the ϵ in $(s'-s-i\epsilon)$ we would get a divergency). As a consequence, we cannot expect that the simple approximation of the integral by the ChPT result will always yield good results.

The main advantage of using the IAM is that we are calculating exactly on the elastic cut, but that is no longer true on the inelastic cuts. Indeed, the method can miss relevant physical features associated to inelastic thresholds. That is indeed the case in pion scattering since, as it can be seen in Table 1, at these energies there is one resonance, the $f_0(980)$, whose nature is closely related to the $K\bar{K}$ threshold.

Taking into account that the inverse amplitude technique is able to reproduce the other two lightest resonances in $\pi\pi$ and πK scattering, it seems very surprising that it is not able to reproduce the $f_0(980)$. Naively, one would expect that, since it works that well up to 900 MeV, just 80 MeV more should not spoil completely the goodness of the approach. However, we will see that there is not even a hint of a resonant behavior in the scalar channel around 985 MeV. One could maybe be tempted to conclude that the IAM only reproduces vector resonances. We do not think this is correct and, indeed, we will see later that we obtain the appropriate analytical structure as far as it is not due to the kaon threshold.

At this point we want to remark the importance of understanding why and when the method does no longer yield the right results. Let us remember that we are also thinking in possible applications of this unitarization procedures to the electroweak chiral effective lagrangian, whose reference model is the Standard Model with a heavy Higgs. In such case, one would expect to see a broad resonance precisely in the scalar channel and we want to have a unitarization procedure that we can trust when it predicts such a resonance.

We do think that the above discussion in terms of inelastic thresholds explains why the IAM fails so abruptly. The reason is not that the ChPT amplitudes become a worse approximation at higher energies, indeed it is connected to the fact that the $f_0(980)$ resonance is related, in a fundamental way, with the kaon threshold.

Nowdays, the $f_0(980)$ resonance parameters are understood in terms, not of a single pole, but two [24, 25]. Once the amplitudes are extended analytically to the whole complex

s plane, the existence of two superimposed cuts on the positive real axis, implies that we have four different Riemann sheets. In our case, the cut produced by the two pion intermediate state is responsible for the appearance of two sheets, which are labelled according to the sign of the center of mass momenta:

$$k_1 \equiv \frac{1}{2}\sqrt{s^2 - 4M_\pi^2} \tag{22}$$

The same happens for the cut produced by two kaon intermediate states, although now the labelling is done with the sign of

$$k_2 \equiv \frac{1}{2}\sqrt{s^2 - 4M_K^2} \tag{23}$$

The usual convention is to label the four sheets by the signs of $(\mathrm{Im}k_1, \mathrm{Im}k_2)$, so that sheet I has $(+,+)$, sheet II $(-,+)$, sheet III $(-,-)$ and sheet IV $(+,-)$. Notice that, with our previous notation, $k_1 \sim \sigma_{\pi\pi}$ and $k_2 \sim \sigma_{K\bar{K}}$, so that a choice of sign for k_1 and k_2 implies a choice of sign for $\sigma_{\pi\pi}$ and $\sigma_{K\bar{K}}$. In this way it is easy to see that the unitarity relation Eq.19 is only satisfied over the right cut when coming from the upper plane in the first sheet. That is the reason why the other sheets are called "unphysical", although they also contain important physical information. Namely, poles can only appear in these sheets and from the point of view of complex analysis, they determine (together with the cut structure) the values of the amplitude at any point of the complex plane. As a matter of fact, resonances are produced by poles located near the real axis, and in the case of $f_0(980)$, it has been shown that its physical parameters can be accomodated with a pole in the second sheet and another one in the third. The first one has been clearly established at $M_{II} = 988 \pm 10 - i(24 \pm 6)$MeV [24]. However, the location of the other pole is not so clear, since it changes considerably depending on how general the representation of the amplitude is taken in the analysis, one finds $M_{III} = 978 - i28$MeV [24] or $M_{III} = 797 - i185$MeV [25].

As we will see later, our approach is not able to reproduce any of these poles. The first one is above kaon threshold and is responsible for the resonance itself. It is located very near the real axis and thus we cannot expect the $\Delta \simeq 0$ ChPT approximation to be valid. Naively one could expect to be able to reproduce the other pole, because its real part is below the kaon threshold. It would have been nice to obtain such a pole in order to shed some light on its real position. Unfortunately, being below the inelastic threshold is not enough, since it is also located on the "unphysical" sheet of the kaon cut, which we are not able to reproduce. From our point of view, these are the reasons why the IAM fails to accomodate the $f_0(980)$ resonance. But the IAM is able to reproduce the other analytical features which are not associated to the kaon inelastic cut. Indeed, we will se in Section 6 that it yields a pole in this channel which, even though it does not produce a resonance, is necessary to describe the experimental data.

3.2.5 $\mathcal{O}(p^4)$ approximation

Throughout the derivation of the IAM we have been using, for simplicity, the chiral amplitudes up to $\mathcal{O}(p^4)$. Nevertheless, it is possible to extend the argument to include higher

order terms, as for instance the $\mathcal{O}(p^6)$ contributions. In that case we would have started from a four times subtracted dispersion relation for the two-loop calculation. Once more, the integral over the right cut would be related to the one for $G(s) = t_{IJ}^{(0)2}/t_{IJ}$. Working out the expansion of the subtraction constants, we would then arrive to

$$t_{IJ} \simeq \frac{t_{IJ}^{(0)2}}{t_{IJ}^{(0)} - t_{IJ}^{(1)} + t_{IJ}^{(1)2}/t_{IJ}^{(0)} - t_{IJ}^{(2)}} \tag{24}$$

which again is nothing but the formal [1,2] Padé approximant, that satisfies exactly the elastic unitarity condition.

As we have commented in the introduction, while we were preparing this work, two new papers have appeared with $\mathcal{O}(p^6)$ calculations of $\pi\pi$ scattering within $SU(2)$ ChPT [4, 5]. We have not used these results, since, as we have already seen, they will not help us to overcome any of the preceeding objections to the IAM. However it is quite likely that, had we used them, the parameters of the fits that we will present in the next sections would had been slightly modified.

4 $\pi\pi$ scattering in $SU(2)$ ChPT

The inverse amplitude method was first applied [8, 14] to $\pi\pi$ scattering without the strange quark. In that case, the massless limit displays an spontaneous symmetry breaking from $SU(2)_L \times SU(2)_R$ to $SU(2)_{L+R}$, which is nothing but the usual isospin. The $\mathcal{O}(p^4)$ expression for $\pi\pi$ scattering was obtained in [2, 26], and it is written in terms of four phenomenological parameters $\bar{l}_1, \bar{l}_2, \bar{l}_3, \bar{l}_4$ as well as the mass and pion decay constants, M_π and F_π that had already appeared in the low energy theorems. In this section we will review how the method is able to reproduce the ρ resonance. We will show some results for recently proposed new parameters in order to test the IAM predictive power, but we will also present a unitarized fit to the data. As a novelty we will use not only the $J = 0$ phase shifts, but also those with $J = 2$, in order to obtain in the best fit with the IAM. In this new calculation, we have also estimated the error bars of the unitarized parameters.

4.1 Results using low-energy parameters

Let us now illustrate what happens if we apply the IAM on the ChPT amplitudes using the values of the chiral parameters obtained only from low energy experiments. It is well known that the IAM is able to extract from this low energy data the right qualitative behavior at high energies, including some resonant states. However, we want to see quantitatively to what extent the main features are reproduced.

In order to simplify the comparison with previous works on the subject, we have chosen $M_\pi = 139.57$ MeV and $F_\pi = 93.1$ MeV. The values of the chiral parameters are not so clear, since in general they have considerable error bars. In Table 2, we have listed the different combinations of parameters and methods that we have taken from the literature to obtain Fig.1.

Method	$\bar{l}_1$	$\bar{l}_2$	M_ρ
ChPT	-0.62±0.94	6.28±0.48	No resonances
Inverse	-0.62±0.94	6.28±0.48	715 MeV
Amplitude	-1.7±1.0	6.1±0.5	675 MeV

Table 2: Sets of parameters and methods used in the text. Those in the first two lines come from K_{l4} decays [27]. Those in the third, from data on K_{l4} and $\pi\pi$ together with some unitarization procedure ref.[28]. M_ρ is calculated with the central values.

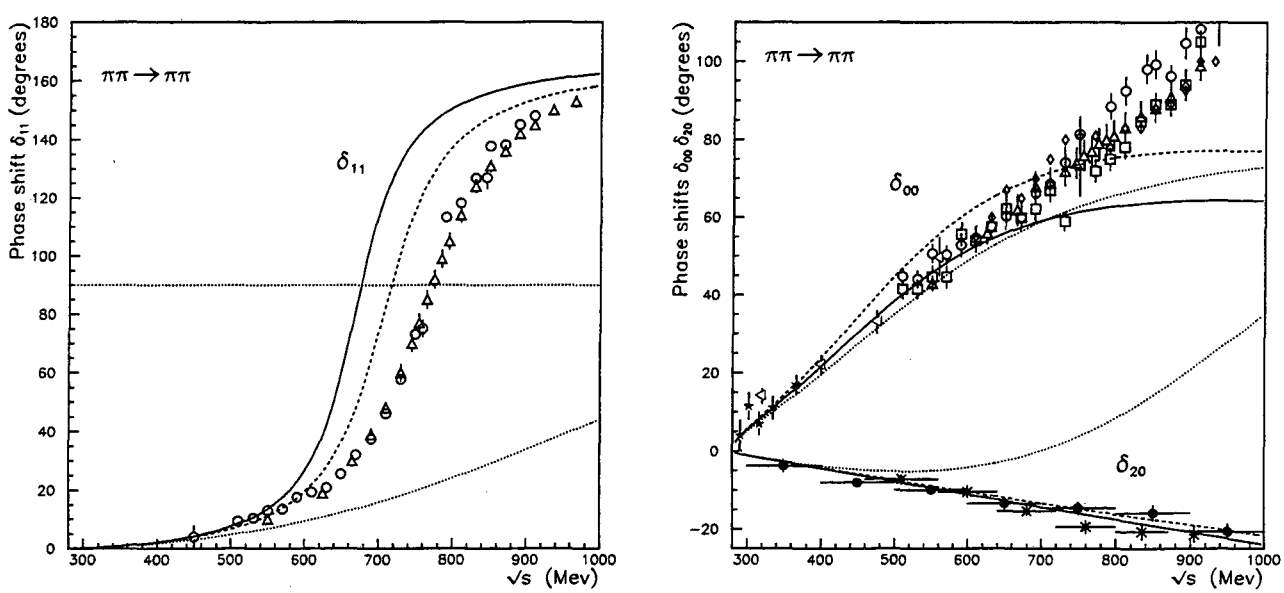

Figure 1.- Phase shifts for $\pi\pi \to \pi\pi$. The dotted curve is plain ChPT with the $\bar{l}_i$ in the first line of Table 2. The other two curves are both the result of the IAM: the dashed one has been calculated again with the same parameters whereas the continuous one corresponds to the $\bar{l}_i$ in the third line of Table 2. The data comes from: [29] ($\triangle$), [30] ($\diamond, \square$), [31] ($\times$),[32] ($\circ$), [33] ($\triangleleft$), [34] ($\star$) and [35] ($\bullet$). The results with $SU(3)$ ChPT would have been exactly superimposed on these curves. The straight line stands at $\delta = 90^0$.

As it had already been shown in [8, 14], from the curves for the $I = 1, J = 1$ channel in Fig.1, it can be clearly seen that the IAM correctly yields a ρ-like resonance. The value of its mass is obtained from the point where the curves cross the $\delta = 90^0$ value and it lies within a 10% to 15% error of its real value. In this way, the ρ resonance can be regarded as a prediction, within that 10% to 15% error, of the IAM with ChPT and the parameters obtained from some low energy data.

It is also evident that the fit of the $I = 2, J = 0$ channel is correct up to much higher energies. In Table 2 we have also included the values of M_ρ corresponding to each choice of parameters. For all the cases we have set $\bar{l}_3 = 2.9, \bar{l}_4 = 4.3$ following reference [2], as it is usual in the literature, since any change in this parameters is related with the actual values of M_π and F_π.

The only feature of $\pi\pi$ scattering that is evidently missing from the unitarized results is the $f_0(980)$ resonance in the $I = 0, J = 0$ channel. As we have already seen in the previous section, this fact is connected with the faliure of the whole approach to properly reproduce the kaon inelastic cut. But let us first obtain a better fit to the data.

4.2 Unitarized fit

Now that we have an amplitude that correctly describes the right cut, while keeping at the same time the correct polynomial form from ChPT, it seems natural to tune the parameters in order to obtain the correct M_ρ [8, 14]. Note that, in principle, fixing the correct mass does not imply that we get a good fit to the data. It could happen that even though the phase shift crosses $\pi/2$ at the right M_ρ, the slope of the curve at that point is incorrect, or in other words, that the width is wrong. In order to differentiate the parameters thus obtained from those coming from plain ChPT we will call them $\hat{l}_1, \hat{l}_2$. With the help of the chiral limit for the (1,1) ChPT amplitude, it is easy to see that this channel is almost only sensible to the following parameter combination: $\bar{l}_1 - \bar{l}_2$. We just then have to tune this combination until we get the M_ρ listed in Table 1. We get: $\hat{l}_1 - \hat{l}_2 = -5.95 \pm 0.02$. In Fig. 2 it can be seen that the results are remarkably succesful. As we will see later, we also get the right ρ width.

Once that difference is fixed, we just have to determine one parameter, say $\hat{l}_2$, and use the $\hat{l}_1 - \hat{l}_2$ value to obtain the other. It is then tempting to try to repeat the same procedure and fix one $\hat{l}_i$ by tuning the $f_0(980)$ mass. In practice, however, we already know that the IAM is not able to reproduce the $f_0(980)$ resonance, so that we will have to determine one of the $\hat{l}_i$ parameters by other means.

In previous studies [8, 14] the unitarized fit to the other phase shifts was used in order to estimate the values of $\hat{l}_1$ and $\hat{l}_2$. But, as it was commented above, the data in the (0,0) channel is not as good as that of (1,1). The same happens for the (2,0) channel, where the curves are not very sensible to small variations in the $\hat{l}_i$ parameters. Therefore, in the present work, we have also used the $J = 2$ channels (mainly the one with $I = 0$) to further constrain the parameter range. Let us remember that for these channels we have $t_{I2}^{(0)} = 0$ and, as we have already discussed in Section 2, the IAM leads again to the ChPT result, although we are now using the $\hat{l}_i$ parameters. That is why we will only use low energy data

Method	$\hat{l}_1$	$\hat{l}_2$	M_ρ (input)	Γ_ρ
Inverse Amplitude	-0.5 $\pm$ 0.6	5.4$\pm$ 0.6	768.8$\pm$ 1.1 MeV	155.6$\pm$1.8 MeV

Table 3: Parameters and results of the one-loop IAM when M_ρ is fixed to its actual value.

in these channels, up to $\simeq$ 600MeV, although in other channels we are using data at higher energies.

Thus, the values given in Table 3 are just a conservative estimate of the range where one parameter, namely $\hat{l}_2$, yields a reasonable fit of the data in the $(I,J) = (0,0), (2,0), (0,2)$ and $(2,2)$ channels. The corresponding values for $\hat{l}_1$ are then obtained from $\hat{l}_1 - \hat{l}_2$. The results are shown in Fig. 2, where the continuous line corresponds to the central $\hat{l}_i$ values and the shaded area to their uncertainties, all them listed in Table 3. Notice that the shaded area has always been obtained by varying just one parameter within its estimated error. Then the other one is fixed from $\hat{l}_1 - \hat{l}_2$.

In Fig.2 it can be seen how it is not possible to fit the $f_0(980)$ resonance with $SU(2)$ ChPT and the IAM. It is clear that, even though the actual value of the δ_{00} phase shift may not lie very far from the unitarized prediction, the qualitative behavior of the curves in this channel is not correct above 800MeV.

With the $\hat{l}_i$ fit we can obtain the total Breit-Wigner width of the ρ resonance from:

$$\Gamma_\rho = \frac{M_\rho^2 - s}{M_\rho} \tan\delta_{11}(s) \tag{25}$$

Indeed we have computed it for different values of s around M_ρ^2 (although not too close since the $\tan\delta$ function is very unstable numerically near the resonance). The result is $\Gamma_\rho = 155.6 \pm 1.8$MeV, which is quite close to the experimental result (see Table 1) and consistent with previous calculations using the IAM (see [8] and references therein). This value is nevertheless slightly high, but we will see that it is possible to obtain the right value when using $SU(3)$ ChPT.

As we have already commented, this result is not at all trivial, since fitting the right mass does not ensure a correct description of the resonance. Therefore, even though we are now using the M_ρ experimental value, the Γ_ρ width is again a prediction of the IAM. Notice, in contrast, that when trying to fit the data by considering explicitly the resonance fields in the lagrangian, one has to introduce both the mass and the width of each resonance. Of course with that procedure one can get extremely good results, even at high energies [9, 10], although the price is a larger number of phenomenological parameters.

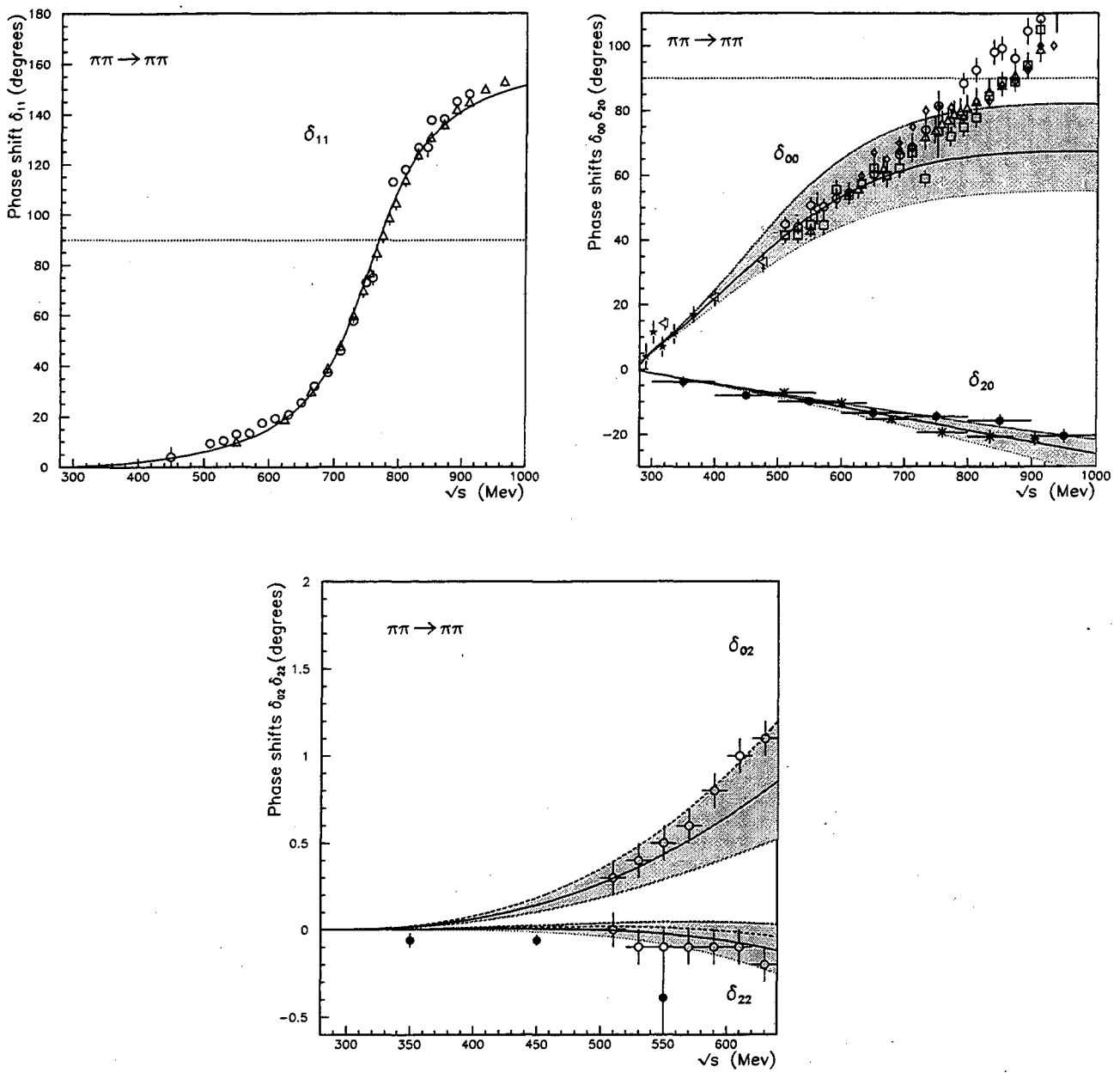

Figure 2.- Pion elastic scattering phase shifts δ_{IJ} obtained from the IAM fit to the correct M_ρ. The shaded areas cover the error bars of the fitted parameters with the constraint $\hat{l}_1 - \hat{l}_2 = -5.95 \pm 0.02$. The dotted straight lines stand at $\delta = 90^0$. Remember that the $J = 2$ partial waves have to be calculated as in plain ChPT. Indeed, the dashed lines in those channels correspond to plain ChPT with the parameteres in the first row of Table 2. The symbols for the experimental data are the same as in Fig.1. The corresponding curves within $SU(3)$ ChPT would almost superimpose.

5 SU(3) Chiral Perturbation Theory

The extension of the ChPT approach to include the strange quark, was done once more, by Gasser and Leutwyler [3]. In this case, there are eight Goldstone bosons, which are identified with the three pions, the four kaons and the eta. In principle it is possible to calculate the amplitudes of any process involving any combination of these particles. However, the breaking of chiral symmetry is larger in the case of the strange quark and thus the masses of the kaons and the etas are larger than M_π. Therefore the thresholds for these reactions are much higher than in pion scattering, which in practice restricts severely the effectiveness of the approach.

Nevertheless, the lowest two particle threshold apart from $\pi\pi$ scattering is that of πK elastic scattering at 630MeV, which is still within the applicability range of ChPT. The calculation of this amplitude to $\mathcal{O}(p^4)$ was performed by Bernard, Kaiser and Meißner [21, 22] who also gave the $\mathcal{O}(p^4)$ result for $\pi\pi$ within $SU(3)$ ChPT. In the literature, these formulae have sometimes appeared with some minor errata which have been corrected in the DAΦNE Physics Handbook [23]. However, even those formulae do not satisfy perturbative unitarity (see Appendix). Following the work in [21] we have rederived an expression which does satisfy that requirement, and we have included it in the Appendix, toghether with a discussion on how it is obtained and its unitarity properties.

In the $SU(3)$ case the phenomenological parameters are the masses of the pseudo-Goldstone Bosons, together with the corresponding decay parameters that, as it is usually done, we have set to:

$$\begin{aligned} M_\pi &= 139.57\text{MeV} \quad M_K = 493.65\text{MeV} \quad M_\eta = 548.8\text{MeV} \\ F_\pi &= 93.1\text{MeV} \qquad F_K = 1.22F_\pi \qquad F_\eta = 1.3F_\pi \end{aligned} \tag{26}$$

There are also twelve one-loop parameters, which now are customarily denoted as $L_i^r(\mu)$ (all them but L_3 and L_7 depend on the renormalization scale [3]). However only a few of them actually contribute to the amplitudes of the processes considered in this section. As a matter of fact, only $L_1^r, L_2^r, L_3, L_4^r, L_5^r, L_6^r, L_8^r$ appear in πK in scattering, whereas in pion scattering only the following combinations are present:

$$2L_1^r + L_3 \qquad L_2^r \tag{27}$$

$$2L_4^r + L_5^r \qquad 2L_6^r + L_8^r \tag{28}$$

Again, and in order to simplify the comparison with previous works, we have fixed the following values:

$$L_4^r(M_\eta) = 0 \quad L_5^r(M_\eta) = 0.0022 \quad L_6^r(M_\eta) = 0 \quad L_8^r(M_\eta) = 0.0011 \tag{29}$$

according to reference [3]. To use a very precise value of these parameters is not very relevant since they are related to the different masses and decay constant that we had already fixed. Hence, in practice, the only relevant parameters for $\pi\pi$ and πK scattering in $SU(3)$ are L_1^r, L_2^r and L_3.

The IAM was first applied to $SU(3)$ ChPT by the authors in [12], were we showed that it is possible to reproduce not only the $\rho(770)$ resonance but also the $K^*(892)$. Our aim in this section is first to to study the predictive power of the method, whether it can accomodate further resonant states, or why it cannot. Then we will present a simultaneous fit to $\pi\pi$ and πK scattering to the ρ and K^* masses. The new features of this analysis is that it uses the corrected ChPT expressions for πK scattering which now truly satisfy perturbative unitarity (see the Appendix) and the fact that we also use the data on the $J = 2$ $\pi\pi$ scattering channels. We will also estimate the error bars on the best fit parameters and we will use it to obtain numerical values for some interesting phenomenological parameters. This fit will also allow us, in section 6, to study the analytical structure of the IAM amplitudes in the complex s plane, as well as to unitarize the $\gamma\gamma \to \pi\pi$ one loop ChPT cross section.

5.1 Results using low energy parameters

Let us then start, as we did in the previous section, with the inverse amplitude results using parameters that have been obtained from low energy data. In Table 4 we list different choices of parameters and methods together with their results for the ρ and K^* masses. As in the case of $SU(2)$ ChPT the IAM is able to predict from low energy data the existence of both resonant states. Remarkably, the masses are obtained again within a 10% to 15% error.

In Fig.3 we show the result of applying the IAM to πK scattering, with the parameters given in Table 4, which have been obtained from low energy data. In contrast with plain $\mathcal{O}(p^4)$ ChPT, it is evident that the IAM is not only able to accomodate the K^* resonance but also to reproduce the right qualitative behavior for the $(I, J) = (3/2, 0)$ channel.

We do not display the results for $\pi\pi$ scattering in $SU(3)$ because they will almost superimpose with those in Fig.1. Indeed, the $\bar{l}_i$ parameters in lines 2 and 3 of Table 2 were obtained, respectively, from the L_1^r, L_2^r, L_3 in lines 2 and 3 of Table 4 [27, 28], by means of:

$$\begin{aligned}
\bar{l}_1 &= 96\pi^2 \left(4L_1^r(M_\eta) + 2L_3 - \frac{\nu_K}{24} - \frac{\nu_\pi}{3}\right) \\
\bar{l}_2 &= 48\pi^2 \left(4L_2^r(M_\eta) - \frac{\nu_K}{12} - \frac{2\nu_\pi}{3}\right) \\
\nu_\alpha &= \log\left(\frac{M_\alpha^2}{M_\eta^2}\right) \quad ; \quad \alpha = \pi, K
\end{aligned} \tag{30}$$

As a matter of fact, we have calculated independently the $\pi\pi$ elastic scattering in $SU(2)$ and $SU(3)$. Using the above equations to relate the parameters in both cases, and below kaon threshold, we have obtained the same results up to numerical differences ($\simeq$1%), which would be unobservable in the figures. That is a nice check of our programs. Therefore, Fig.1 is also the result for $\pi\pi$ scattering in the $SU(3)$ formalism, but now with the parameters in Table 4.

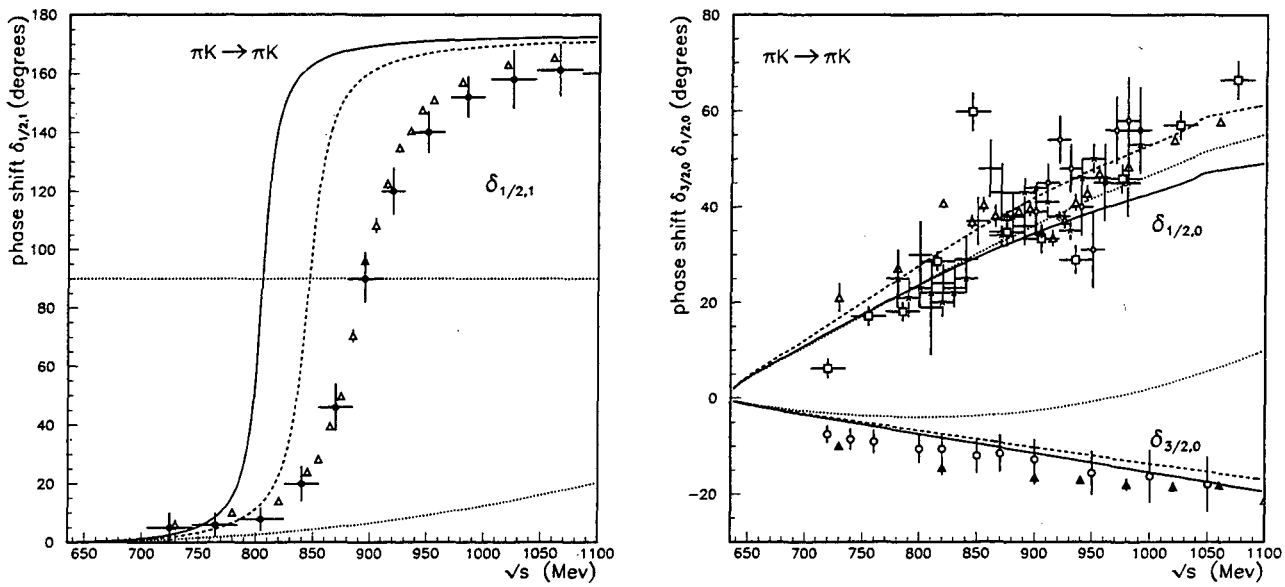

Figure 3.- Phase shifts for elastic πK scattering. The dotted curve is plain ChPT with the L_i parameters in the first line of Table 4. The other two curves are both obtained from the IAM: the dashed one again with the same parameters and the continuous one with those in the third line of Table 4. The experimental data comes from:[36] (•), [37] (⋆), [38] (∘), [39] (◇), [40] (□) and [41] (△). The straight dotted line stands at $\delta = 90^0$.

Method	$L_1^r(M_\eta) \cdot 103$	$L_2^r(M_\eta) \cdot 103$	$L_3 \cdot 103$	M_ρ	M_{K^*}
ChPT	0.65±0.28	1.89±0.26	-3.06±0.92	-	-
Inverse	0.65±0.28	1.89±0.26	-3.06±0.92	717 MeV	847 MeV
Amplitude	0.6±0.3	1.75±0.3	-3.5±1.1	680 MeV	804 MeV

Table 4: Different sets of parameters and methods used in the text. Those of the first two lines come from K_{l4} decays [27]. Those of the third line come from data on K_{l4} and $\pi\pi$ together with some unitarization procedure (for details see ref.[28]). The quoted values of M_ρ and M_{K^*} are calculated with the central values.

5.2 Unitarized fit

As it happened in the $SU(2)$ case, we now have an expression for the amplitude that behaves correctly with respect to unitarity and that presents the right form in the low energy limit. Therefore, we can try to use the actual $\rho(770)$ and $K^*(892)$ masses, given in Table 1, in order to get a good parametrization of $\pi\pi$ and πK phase shifts. Once again we remark that nothing ensures that fitting the right masses will give us the right description of phase shifts, since, among other things, the widths of the resonances could be wrong.

When dealing with the $SU(3)$ chiral lagrangian we have more parameters and the way they appear in the amplitudes is more complicated. Let us first start with the $\pi\pi$ scattering partial waves in $SU(3)$. As we have already commented, they only depend on $2L_1^r + L_3$ and L_2^r. Even more, the (1,1) channel only depends on $2L_1^r + L_3 - L_2^r$, (which is renormalization scale independent) and will be fixed with M_ρ. Once more and in order to avoid confusions with the ChPT low-energy parameters, we will denote the paremeters of our fit by $\hat{L}_i^r$.

Let us then start by fixing the $\rho(770)$ mass to its actual value. In so doing we get

$$2\hat{L}_1^r + \hat{L}_3 - \hat{L}_2^r = (-3.11 \pm 0.01)10^{-3} \tag{31}$$

As a consistency check we see that it is within a 1% of $-3.14\ 10^{-3}$ which is obtained from the $\hat{l}_i$ parameters of the $SU(2)$ case, with the help of Eq.30.

Using the value in Eq.31, it is enough to determine $\hat{L}_2^r$ in order to extract $2\hat{L}_1^r + \hat{L}_3$, in complete analogy with the $SU(2)$ case. Once again we use the other channels $(I, J) = (0,0), (2,0), (0,2)$ and $(2,2)$ to determine the best $\hat{L}_2^r$ value, which indeed is the same that we would have obtained from the $\hat{l}_2$ $SU(2)$ parameter by means of Eq.30. It can be found in Table 5. Hence, the best $SU(3)$ fit of the $\pi\pi$ phase shifts, yields almost the same results as those obtained with $SU(2)$. In practice, the very same Fig.2 remains valid for $SU(3)$ and that is why we are not displaying it twice. Nevertheless, when computing the M_ρ within the $SU(3)$ formalism, we obtain a much better value than in $SU(2)$, which was about 5 MeV too high. It is also listed in Table 5.

Up to the moment we have just determined $\hat{L}_2^r$ and $2\hat{L}_1^r + \hat{L}_3$. In order to obtain $\hat{L}_1^r$ and $\hat{L}_3$ separately, we simply have to fix the correct $K^*(892)$ mass in the $I = 1/2, J = 1$ πK channel, by varying the $\hat{L}_3$ value. However, the $K^*(892)$ has an added subtlety when compared with the $\rho(770)$, namely, that the mass splitting between charged states is of the order of 5 MeV. This is an small isospin breaking effect that we have not included in our approach. Therefore, we have used an average mass $\overline{M}_{K^*} = 894.0 \pm 2.5$ MeV with an error bar that includes the mass of any $K^*(892)$ state, no matter what its charge may be. That uncertainty has also been taken into account in the $\hat{L}_i^r$ error estimates.

Once we have $\hat{L}_3$, we use $\hat{L}_2^r$ and Eq.27 to obtain $\hat{L}_1^r$. The parameters of this fit have been collected in Table 5, together with Γ_ρ and Γ_{K^*}, which can be considered as predictions of the approach. Notice, however, that in this case, the width of the $K^*(892)$ resonance is obtained only up to a 20% error, which nevertheless we consider a reasonably good result in view of the whole fit in that channel.

Concerning the parameters, it can be noticed that, as expected, they do not lie very far from those in Table 4, which were obtained from low energy data. Indeed, they are

Method	$\hat{L}_1^r(M_\eta)\cdot 10^3$	$\hat{L}_2^r(M_\eta)\cdot 10^3$	$\hat{L}_3\cdot 10^3$	Γ_ρ	Γ_{K^*}
Inverse Amplitude	0.41±0.20	1.48 ± 0.33	-2.44± 0.21	149.9± 1.2 MeV	41.2 ± 1.9 MeV

Table 5: Parameters and results of the $SU(3)$ IAM when $M_\rho = 768.8 \pm 1.1$MeV and $\overline{M}_{K^*} = 894.00 \pm 2.5$ MeV are fixed to their actual values. Notice that for $K^*(892)$ we have chosen an average mass between its different charge states.

compatible inside the error bars. Even more, they also seem to be consistent with other parameters that have been obtained from the IAM applied to the form factors of the $K \to \pi\pi l\nu$ decays [13], which are very well know experimentally:

$$\hat{L}_1^r(M_\eta) = (0.74 \pm 0.14)10^{-3} \quad \hat{L}_2^r(M_\eta) = (1.07 \pm 0.18)10^{-3} \quad \hat{L}_3(M_\eta) = (-2.45 \pm 0.52)10^{-3} \tag{32}$$

(notice that in that reference they are using slightlly different definitions, as $F_K = F_\pi$, so that the parameters do necessarily differ. See also the Appendix.)

Nevertheless, it would not make any sense to try to reduce the error bars of these parameters. We consider that the approach that we have been following here can only be consistent within a few percent error level. If one would like to have a better accuracy it would be necessary to take into account higher order ChPT corrections, probably electromagnetic effects (at least for the mass splittings) and the whole approach should be modified following the comments that we made in previous sections.

In Fig.4 we show the results of the $SU(3)$ IAM fit to the resonance masses, in terms of elastic scattering phase shifts, which we think deserve some comments:

- First notice that, again, we are not showing the curves for $\pi\pi$ scattering since they are exactly those in Fig.2. The differences only appear above the two kaon threshold, since in the $SU(3)$ formulae we are also considering internal loops of kaons and etas, which modify the unitarity condition. Indeed, we have also computed the phase shifts with the IAM, but obtaining the imaginary part of the amplitude above threshold from the modified unitarity condition in Eq.19. There is no improvement in the results. That should be expected from the discussion in Section 3.2.1, since such a procedure does not reproduce the $K\bar{K}$ cut. Hence, the $f_0(980)$ resonance is out of reach even with this "improved" approach.

- In the $\pi K \to \pi K$ case we can extend the graphs up to 1100 MeV, or even more, since the first inelastic threshold is $K\eta$ production at 1040 MeV and, in contrast to the $\pi\pi$ case, there is no nearby resonance. Indeed, the next resonant state in πK elastic scattering is $K_0^*(1430)$, very high to affect dramatically our results at 1100 MeV, but also to be correctly reproduced by the IAM method. Nevertheless, the existence of the $K\eta$ threshold can be noticed in the $I = 1/2, J = 0$ channel, as a small bump in the curves at precisely 1040 MeV.

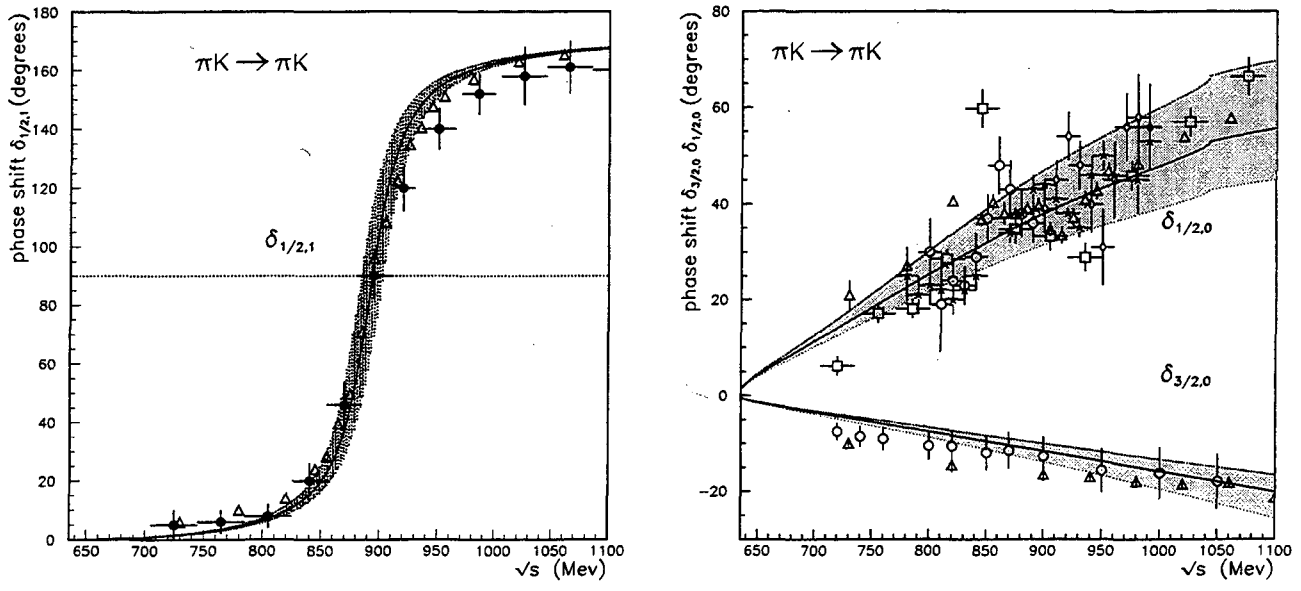

Figure 4.- πK elastic scattering phase shifts δ_{IJ} obtained from the IAM fit to the correct M_ρ and M_{K^*}. The shaded areas cover the error bars of the fitted parameters with the constraint $2\hat{L}_1^r + \hat{L}_3 - \hat{L}_2^r = (-3.11 \pm 0.01)10^{-3}$. The dotted straight line stands at $\delta = 90^0$. The symbols for the experimental data are the same as in Fig.3.

- The shaded area in the $K^*(892)$ channel is not only due to the averaged mass for $K^*(892)$ with 2.5MeV error, but also to the fact that we have to determine several parameters to get the right mass, in contrast with the $\rho(770)$ case, when we only had to fix one.

Obviously, the calculation for πK scattering cannot be checked with $SU(2)$ as we did for $\pi\pi \to \pi\pi$. However, we have explicitly checked that the ChPT amplitudes that we obtain satisfy perturbative unitarity. As it is explained in the Appendix, previous calculations [22, 12], including ours, did not respect this condition, although by a very small amount. That is why the values of the best parameters for this fit are slightly different those of our previous work [12].

Phenomenological parameters

Once we have a good parametrization of $\pi\pi$ and πK elastic amplitudes, we can use it to obtain the values of some relevant phenomenological parameters. First we can calculate the scattering lengths, which determine the strength of the interactions at low energy. Despite our IAM fit makes use of high energy data, we expect that it will reproduce the low energy behavior since in the low energy limit it reduces to the chiral expansion, which at $\mathcal{O}(p^4)$ already yields quite good values (see Tables 6 and 7). However, as far as the IAM is

non-perturbative we are also taking into account higher order effects, that will modify the numerical results. Indeed, some of these lengths have already been calculated with the IAM and it yields slightly better results than plain ChPT [13]. We have made again the calculation with our fit, but as far as we have an estimate of the error bars in the $\hat{L}_i$ parameters, we will be able to give theoretical error estimates for the scattering lengths and the slope parameters (they are mostly dominated by the error in $\hat{L}_2$).

Before giving the results, it is convenient to recall that usually the definition of the scattering lengths is used with two different normalizations. Namely:

$$\mathrm{Re}t_{IJ}(s) = q^{2J}\left(a_J^I + b_J^I q^2 + \mathcal{O}(q^4)\right) \tag{33}$$

for $\pi\pi$ scattering, where q is the C.M. momentum $q^2 = s/4 - M_\pi^2$, and

$$\mathrm{Re}t_{IJ}(s) = \frac{\sqrt{s}}{2} q^{2J}\left(a_J^I + b_J^I q^2 + \mathcal{O}(q^4)\right) \tag{34}$$

for πK scattering, where now $q^2 = [s - (M_K + M_\pi)^2][s - (M_K - M_\pi)^2]/4s$.

Finally, the predictions of our fit for the $\pi\pi$ and πK scattering lengths are given in Tables 6 and 7. Notice that they are expressed in units of M_π in order to compare with previous results. As it can be seen in these tables, all the values are compatible with experimental data, and in general they only differ very slightly from the $\mathcal{O}(p^4)$ ChPT results, usually in the right direction toward the central value. However, the experimental error bars are still too big to arrive to any conclussion. Nevertheless, very recently it has appeared a two loop calculation of $\pi\pi$ scattering within SU(2) ChPT, that estimates $a_0^0 \sim 0.217$ or 0.215 and $a_0^0 - a_0^2 \sim 0.258$ or 0.256, which are precisely the values obtained with our IAM fit. This fact gives support to the idea that the IAM somehow takes into account higher order terms even at low energies.

We have also calculated the phase of the ϵ' parameter, which measures direct CP violation in $K \to \pi\pi$ decays [43]. It is related to the s-wave phase shifts as follows:

$$\phi(\epsilon') = 90^o - (\delta_0^0 - \delta_0^2)_{s=M_{K^0}^2} \tag{35}$$

Our result is:

$$\phi(\epsilon') = 42^{-7}_{+5} \tag{36}$$

very close to $\phi(\epsilon') = 45 \pm 6^o$ which is obtained in plain ChPT [44].

Finally, in Fig.5 we show the phase difference $\delta_{00} - \delta_{11}$, compared with the hitherto available experimental data [34]. The difference between the IAM and plain ChPT at high energies is due to the presence of the ρ resonance. Nevertheless, there are also some differences at low energies, since the dispersive approach is somehow taking into account higher order contributions. It is expected that in the near future, there will be much more precise data coming from K_{l4} decays at DAΦNE and Brookhaven [6, 23].

a_J^I	ChPT	IAM fit	Experiment
a_0^0	0.201	0.216 ± 0.008	0.26 ± 0.05
b_0^0	0.26	0.289 ± 0.025	0.25 ± 0.03
a_0^2	-0.041	-0.0417 ± 0.0014	-0.028 ± 0.012
b_0^2	-0.070	-0.075 ± 0.003	-0.082 ± 0.008
a_1^1	$3.6 \cdot 10^{-2}$	$(3.744 \pm 0.002)\cdot 10^{-2}$	$(3.8 \pm 0.2)\cdot 10^{-2}$
b_1^1	$0.43\cdot 10^{-2}$	$(1.546 \pm 0.003)\cdot 10^{-2}$	-
a_2^0	$20 \cdot 10^{-4}$	$(17.1 \pm 3.5)\cdot 10^{-4}$	$(17 \pm 3)\cdot 10^{-4}$
a_2^2	$3.5 \cdot 10^{-4}$	$(2.8 \pm 1.5)\cdot 10^{-4}$	$(1.3 \pm 3.1)\cdot 10^{-4}$

Table 6: $\pi\pi$ scattering lengths. The ChPT results are taken from [27]. The experimental data comes from [42]

a_J^I	ChPT	IAM fit	Experiment
$a_0^{3/2}$	-0.043	-0.049 ± 0.004	-0.13...-0.05
$b_0^{3/2}$	-	-0.026 ± 0.003	-
$a_0^{1/2}$	0.148	0.155 ± 0.012	0.13...0.24
$b_0^{1/2}$	-	0.087 ± 0.016	-
$a_1^{1/2}$	0.012	0.0146 ± 0.0012	0.017...0.018

Table 7: πK scattering lengths. Note that the ChPT results heve been obtained using the corrected formulae in the Appendix. The experimental data comes from [21]

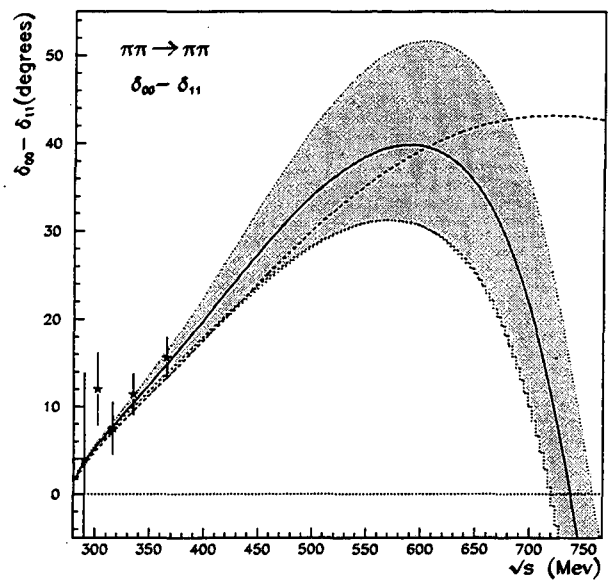

Figure 5.- $\delta_{00} - \delta_{11}$ phase shift difference from the IAM fit (solid line) and plain ChPT (dashed line). The shaded area covers the uncertainty in the $\hat{L}_i$ parameters and the data comes from [34].

6 The IAM in the complex s plane

One of the main objections to unitarization procedures is the apparent arbitrariness in their predictions, which may differ from one another. In most cases, this methods are nothing but a small modification of the amplitudes so that they can satisfy the unitarity constraint in Eq.4, while keeping at the same time the good low energy behavior. But that constraint is not enough to determine the amplitude completely, so that there are as many unitarization techniques as algebraic tricks to implement such a constraint exactly or to get a better approximation.

However, we have already seen in Section 3.1 that, below any other inelastic threshold, the inverse amplitude method can be derived directly from the analytic structure of the general two body elastic scattering amplitude. Our purpose in this section is to show that indeed, apart from satisfying elastic unitarity, it provides the correct analytic structure of the amplitudes that is required from relativistic Quantum Field Theory. Such an structure is not trivial at all and cannot be reproduced by other unitarization procedures. Both the left and right unitarity cuts are already present in plain ChPT, therefore, we will mainly focus on the other relevant features of analyticity. Namely, that poles can only occur in the second Riemann sheet, and that all resonances have to be related to such poles in the vicinity of the real s axis.

In the previous section we used the most naive criteria to identify resonances, i.e., that

the phase crosses the $\delta = 90^0$ value. However, that is only true for the cleanest cases and in general to find $\delta = 90^0$ does not imply the existence of a resonant state. One just have to look at the $\pi\pi$ $I = 0, J = 0$ phase shift data in Fig.2 and notice that even though it obviously crosses $\delta = 90^0$ at about 750 to 850 MeV, the first resonance in that channel, $f_0(980)$, is usually placed at higher energies.

As a matter of fact the existence of a resonance is reflected in scattering processes as a sudden and considerable variation in the phase shift, a rather vague definition. As we have already commented, the rigorous characterization of resonances is made in terms of poles in the second Riemann sheet of the amplitudes in the s complex plane. Indeed, when a resonance is produced by just one of these poles, both its mass and width can be related to the pole position by:

$$E_R \equiv \sqrt{s_{pole}} \simeq M_R + i\frac{\Gamma_R}{2} \tag{37}$$

provided the width is small enough. In case the resonance is due to more poles, the relation is slightly more complicated, but the resonance physical parameters can also be obtained from the position of the poles [24]. The most realistic case is when the pole is not responsible for the whole phase in the real axis, but there is also a so called background phase contribution. That is indeed what happens with the $f_0(980)$ resonance whose poles yield an steep rise in the phase shift over an existing background $\delta \simeq 90^0$ [24, 25].

In this work we have extended analytically to the s complex plane both the $\pi\pi$ and the πK elastic scattering amplitudes, that are obtained with the IAM applied to one-loop $SU(3)$ ChPT. Notice that the cuts in ChPT come from logarithmic functions, so that we have infinite sheets in the complex plane. However, only two of them correspond to the first and second Riemann sheets that any amplitude cut should present. Once we have identified these sheets we can check whether the resonances that we found in previous sections are produced by a pole in the second Riemann sheet and thus whether they have a real sound basis.

We will first analyze the $\pi\pi \to \pi\pi$ process. In Figure 6 we represent the imaginary part of the amplitude in the complex s plane for the three channels $(I, J) = (0,0), (1,1)$ and $(2,0)$. Notice that when we say complex s plane, we mean that we have parametrized s as $s = (E + iC)^2$, where E is the CM energy and is represented in the real axis whereas C provides the complex part. (In this way the plots are actually showing the amplitudes on the $\sqrt{s}$ plane, but in this way the units are easier to interpret. Anyway we will keep on calling it the complex s plane). On the left column we have displayed the results in the first Riemann sheet, whereas the second is represented in the right column. In all cases it can be clearly noticed the existence of a cut on the real axis on the first Riemann sheet. As we had commented before, a right cut is not anything completely new, since it is already present in one-loop ChPT, although in that case, the values that the amplitudes take on it are different. In contrast, the most striking new feature in the IAM amplitudes is the appearance of poles in the second Riemann sheet and how they determine the amplitude shape for the physical values of s.

Indeed, we have found two poles with $\mathrm{Im}s < 0$ in the second Riemann sheet, one in the

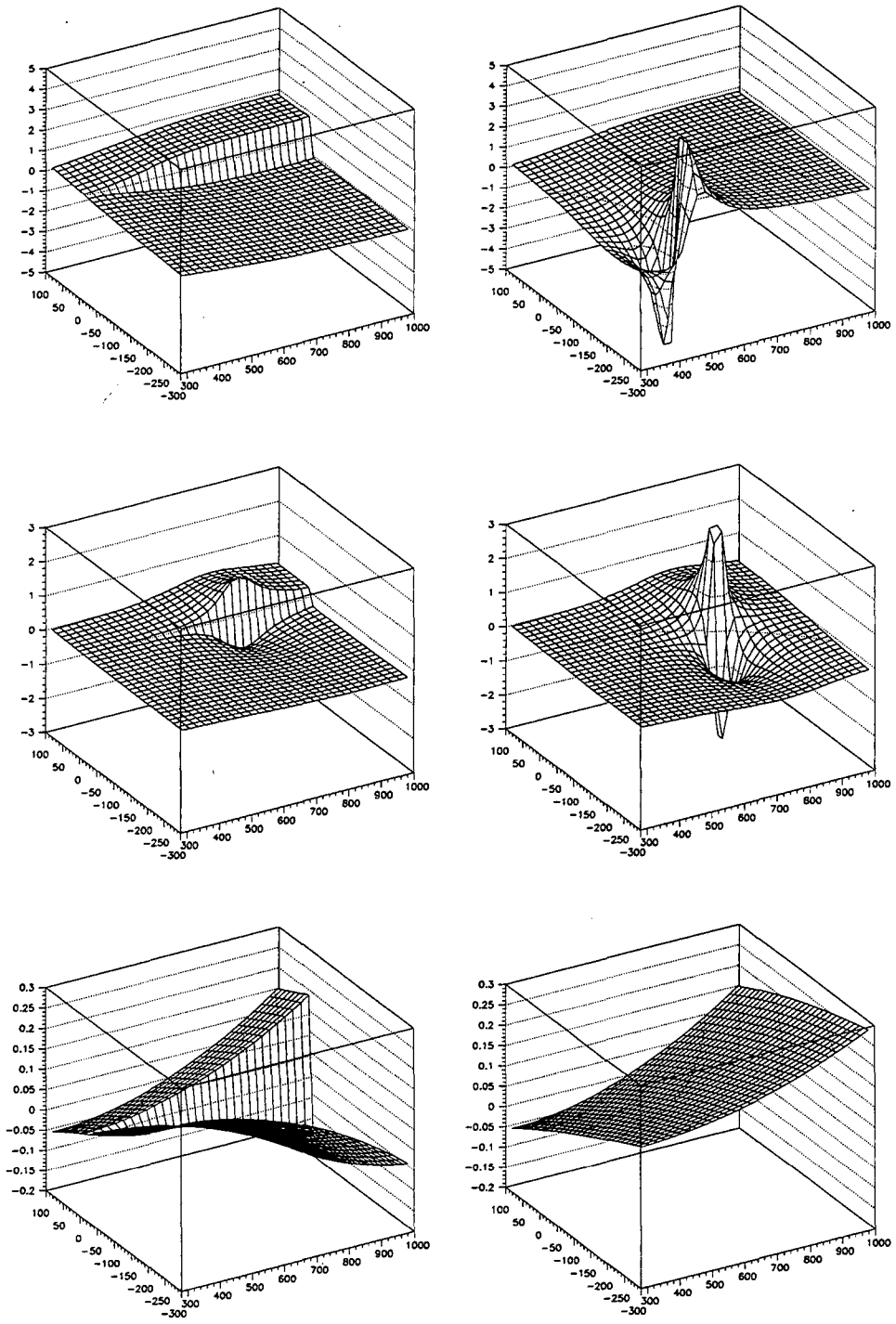

Figure 6.- Imaginary parts of the $\pi\pi \to \pi\pi$ amplitudes in the complex s plane. The first row is the $(I, J) = (0, 0)$ channel, the second is $(1, 1)$ and the bottom is $(2, 0)$. The left plots correspond to the first Riemann sheet, and those on the right, to the second.

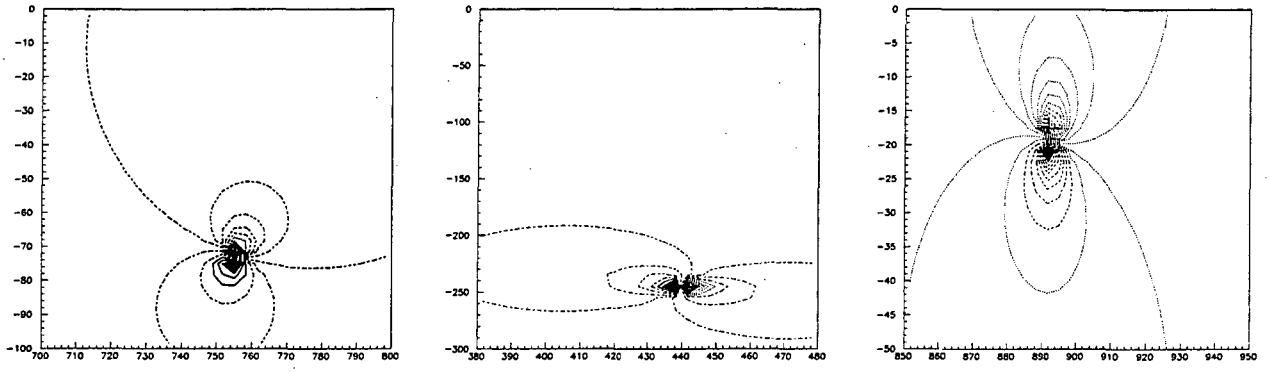

Figure 7.- Contour plots of the second Riemann sheets for different $SU(3)$ ChPT unitarized amplitudes. From left to right they correspond to the $(1,1)$ and $(0,0)$ $\pi\pi$ scattering channels and the $(1/2,1)$ $\pi K \to \pi K$ channel.

$(0,0)$ partial wave and another one in $(1,1)$. Let us start with the second, which clearly corresponds to the ρ resonance. The position of this pole can be obtained from the contour plots in Figure 7, and it is found at around $E_R \sim 760 - i75$. Using Eq.37 we see that it is in a good agreeement with the $\rho(770)$ mass and width parameters given in Table 1. Therefore, we can conclude that the prediction of the IAM for the $\rho(770)$ resonance is completely consistent.

The other pole that can be seeen in $\pi\pi \to \pi\pi$ is on the $(0,0)$ channel. Using the parameters of the best $SU(3)$ IAM fit of the previous section, we find that it is located at $E_R \sim 440 - i245$. This pole is not responsible for the appearance of any resonance, since it is very far away from the real axis. However, from purely phenomenological fits to pion scattering data it had already been pointed out the existence of such a pole around $E_R \sim 408 - i342$ MeV [25]. This pole is responsible for the strong interaction in the $(0,0)$ channel that dominates at low energy the two pion interaction. We can now see that even in the channel where there is not an apparent improvement, the IAM yields the correct analytical structure.

Much as it happened in previous sections, the method is not able to reproduce the $f_0(980)$ resonance. As we already commented, this resonance is now believed to be caused by two poles: one in the second Riemann sheet, but above the two kaon inelastic threshold and the other one below, but in the third Riemann sheet. Following the same steps as before, we have also identified these sheets in the $\pi\pi \to \pi\pi$ amplitudes and we have been able to take a look at all the sheets in search of more poles. Indeed, we have even implemented the IAM derived with the inelastic unitarity condition in section 3.2.4. We have not found any pole that could hint the existence of such resonance. As we have already explained, we should not expect to find anything since the approach is not able to reproduce properly the two kaon unitarity cut and consequently neither its associated sheet structure.

Let us now address to the πK elastic scattering case. Again, in Fig.8 we have displayed

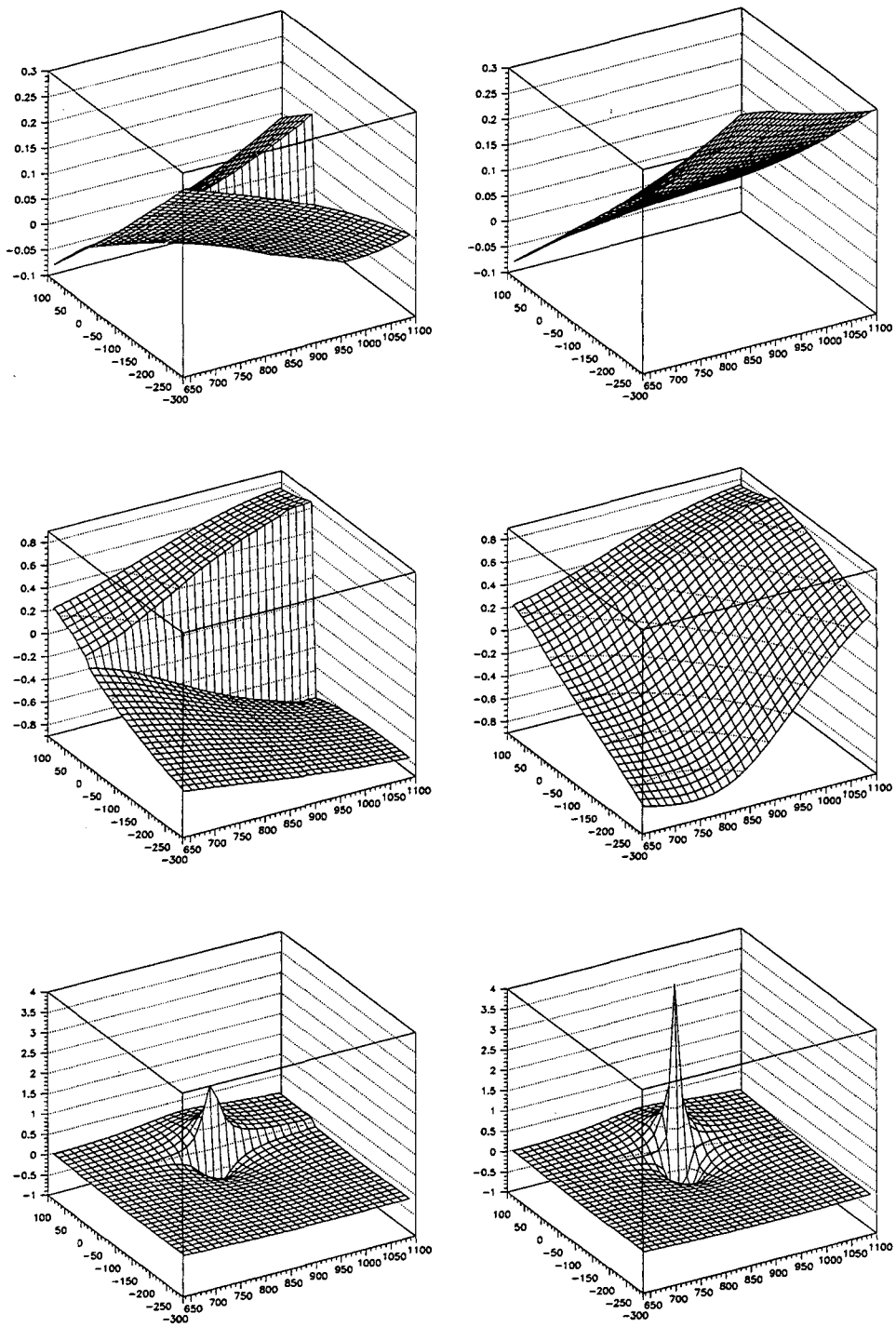

Figure 8.- Imaginary parts of the $\pi K \to \pi K$ IAM amplitudes in the complex s plane. The first row is the $(I, J) = (3/2, 0)$ channel, the second is $(1/2, 0)$ and the bottom is $(1/2, 1)$. Again, the left plots correspond to the first Riemann sheet, and those on the right, to the second.

the imaginary part of the amplitudes for the $(3/2,0),(1/2,0)$ and $(1/2,1)$. Those pictures on the left represent the first Riemann sheet and those on the right, the second. Once more it is clear the existence of a unitarity cut, but also the appearance of a pole in the appropriate channel. In particular, using the third contour plot of Fig.8, we have found a pole in $E_R \sim 890 - i20$ MeV, which using Eq.37 yields again the mass and width for the $K^*(892)$ resonance that we gave in Table 5.

7 Conclusions

In this work we have shown how the IAM provides a consistent technique to accomodate resonances. Indeed, based on its derivation from Dispersion Theory, we have made a systematic analysis of its applicability constraints. We have found that it is mainly limited by the existence of inelastic thresholds and by the fact that the tree level approximation vanishes in some channels.

We have found that its predictive power, once the chiral parameters are determined from low energy data, is of the order of 15% for the masses and widths of the resonances. We think this fact gives a sound basis for its application to the strongly interacting symmetry breaking sector.

Moreover, once we force the IAM results to fit the actual resonance mass values, we get a remarkably good fit to data which is able to reproduce the experimental data up to the next relevant inelastic threshold. Following that procedure, we have given the unitarized $SU(2)$ ChPT fit to $\pi\pi \to \pi\pi$ as well as that of $SU(3)$ to $\pi\pi$ and πK elastic scattering. For the first time we have estimated the values of the unitarized chiral parameters together with their error bars. These values do not lie very far from those obtained without the IAM, and therefore do not spoil the low energy expansion, as can be noticed from the scattering lengths that we have given.

We consider that it would not make any sense to try to reduce the error bars in the unitarized parameters within this approach. One has to keep in mind that we have neglected higher order ChPT corrections, electromagnetic effects, and that we have used high energy data which is very sensible to such effects. It is quite likely that, in order to obtain results consistent to a higher degree of accuracy, the IAM in the simple version that has been used here, will not be enough.

Finally we have also shown how the IAM yields the proper analytic structure in the complex s plane, in contrast with other unitarization techniques. Indeed, we have found that the apparent resonant behavior that is observed on phase shifts, is produced by the corresponding poles in the second Riemann sheet, meeting the strict requirements imposed by general relativistic Quantum Fiel Theory.

Therefore, we think that the IAM and unitarization by means of dispersion theory is the most natural and economic way to extend the applicability of ChPT. We have seen however, that its main limitations come from the existence of inelastic thresholds. Nevertheless, work is still in progress in the subject, the IAM has been recently applied to other processes and higher order ChPT calculations will be soon available. As far as some other physically

relevant features do not lie very far from the present applicability limits, it seems very likely that they can be reproduced in the near future.

Acknowledgments

J.R.P would like to thank the Theory Group at Berkeley for their kind hospitality and M.S.Chanowitz for calling his attention on the f_0 problem. He also wishes to thank the Jaime del Amo Foundation for a fellowship. We have also profited from discussions with U.-G. Meißner on the πK elastic scattering amplitudes. This work has been partially supported by the Ministerio de Educación y Ciencia (Spain) (CICYT AEN93-0776). Partial support by US DOE under contract DE-AC03-76SF00098 is gratefully acknowledged.

A Elastic scattering amplitudes in $SU(3)$ ChPT and Unitarity

As we have already commented in the text, the chiral lagrangian formalism was extended to include the strange quark by Gasser and Leutwyler [3]. Nevertheless, the calculation of elastic πK scattering was later performed in [21]. These amplitudes were given in terms of physical as well as *lowest order* masses and decay constants, which are usually denoted by M_P, F_P and M_P^0, F^0, respectively (P being either π, K or η). Of course, the only mesurable parameters are the first, and when comparing with experimental observations, one has to eliminate those from *lowest order* in terms of the physical constants.

Indeed, it is possible to find [3] the relation between M_π^0 and M_π as well as that between M_K^0 and M_K. Unfortunately, at *lowest order* there is only one F^0, which is related both to F_π and F_K. Hence, whenever one finds F^0 in an expression there are two choices: either relate it to F_π or to F_K. The difference between the two choices will be one order higher in the chiral expansion. For instance, if one has an $\mathcal{O}(p^2)$ expression with F_0^2, in principle one can substitute it by F_π^2, F_K^2 or $F_\pi \cdot F_K$. All these choices are the same up to $\mathcal{O}(p^4)$. When one is working only with pions, the natural choice is the one that leaves all the expressions in terms of F_π, but when one is dealing both with pions and kaons, it is not so obvious. However, we have found that some of these choices lead to a violation of perturbative unitarity, i.e:

$$\mathrm{Im}t^{(1)} = \sigma_{\alpha\beta} t^{(0)\ 2} \tag{38}$$

Surprisingly, the usual choice in the literature [22] which is the one we had also chosen in our previous work on $SU(3)$ unitarization [12], does not satisfy this constraint. This fact can be easily checked by counting the powers of F_π and F_K in the tree level and $\mathcal{O}(p^4)$ results. Indeed, there is a factor F_K^2/F_π^2 of difference between both sides of the above equation. Numerically that amounts to a $(1.22)^2 \simeq 1.5$ factor.

Thus, we have rederived from the original work [21] the amplitudes in terms of physical

quantities, so that they satisfy perturbative unitarity. The result is:

$$
\begin{aligned}
T^{3/2}(s,t,u) &= \frac{M_\pi^2+M_K^2-s}{2F_\pi F_K} + T_4^T(s,t,u) + T_4^P(s,t,u) + T_4^U(s,t,u) + \mathcal{O}(s^3) \qquad (39)\\
T_4^T(s,t,u) &= \frac{1}{16F_\pi F_K}(M_\pi^2-M_K^2)(3\mu_\pi - 2\mu_K + \mu_\eta)\\
T_4^P(s,t,u) &= \frac{2}{F_\pi^2 F_K^2}\Big\{4L_1^r(t-2M_\pi^2)(t-2M_K^2) + 2L_2^r\left[(s-M_\pi^2-M_K^2)^2 + (u-M_\pi^2-M_K^2)^2\right]\\
&+ L_3^r\left[(u-M_\pi^2-M_K^2)^2 + (t-2M_\pi^2)(t-2M_K^2)\right] + 4L_4^r\left[t(M_\pi^2+M_K^2) - 4M_\pi^2M_K^2\right]\\
&+ 2L_5^r M_\pi^2(M_\pi^2-M_K^2-s) + 8(2L_6^r+L_8^r)M_\pi^2M_K^2\Big\}\\
T_4^U(s,t,u) &= \frac{1}{4F_\pi^2F_K^2}\Big\{\frac{3}{2}\Big[(s-t)\left(L_{\pi K}(u)+L_{K\eta}(u) - u\left(M_{\pi K}^r(u)+M_{K\eta}^r(u)\right)\right)\\
&+ \left(M_K^2-M_\pi^2)^2(M_{\pi K}^r(u)+M_{K\eta}^r(u)\right)\Big] + t(u-s)[2M_{\pi\pi}^r(t)+M_{KK}^r(t)]\\
&+ \frac{1}{2}(M_K^2-M_\pi^2)[K_{\pi K}(u)(5u-2M_K^2-2M_\pi^2) + K_{K\eta}(u)(3u-2M_K^2-2M_\pi^2)]\\
&+ \frac{1}{8}J_{\pi K}^r(u)\left[11u^2 - 12u(M_K^2+M_\pi^2) + 4(M_K^2+M_\pi^2)^2\right] + +J_{\pi K}^r(s)(s-M_K^2-M_\pi^2)^2\\
&+ \frac{3}{8}J_{K\eta}^r(u)\left(u-\frac{3}{2}(M_K^2+M_\pi^2)\right)^2 + \frac{1}{2}J_{\pi\pi}^r(t)t(2t-M_\pi^2) + \frac{3}{4}J_{KK}^r(t)t^2\\
&+ \frac{1}{2}J_{\eta\eta}^r(t)M_\pi^2\left(t-\frac{8}{9}M_K^2\right)\Big\}
\end{aligned}
$$

The functions $M_{PQ}, L_{PQ}, K_{PQ}, J_{PQ}, \mu_P$, with $P,Q = \pi, K, \eta$, can be found in [3] although they should be written in terms of physical quantities.

We have verified analytically that this amplitude satisfies the perturbative unitarity constraint. Moreover, we have used that constraint as a check of our programs.

For completeness, we will also give the $SU(3)$ formulae used in this work for $\pi\pi$ scattering, because they have also appeared with some minor errata in the literature:

$$
\begin{aligned}
A(s,t,u) &= \frac{(s-M_\pi^2)}{F_\pi^2} + B(s,t,u) + C(s,t,u) + \mathcal{O}(s^3) \qquad (40)\\
B(s,t,u) &= \frac{1}{F_\pi^4}\Big\{\frac{M_\pi^4}{18}J_{\eta\eta}^r(s) + \frac{1}{2}(s^2-M_\pi^4)J_{\pi\pi}^r(s) + \frac{1}{8}s^2J_{KK}^r(s)\\
&+ \frac{1}{4}(t-2M_\pi^2)^2J_{\pi\pi}^r(t) + t(s-u)\left[M_{\pi\pi}^r(t) + \frac{1}{2}M_{KK}^r(t)\right] + (t\leftrightarrow u)\Big\}\\
C(s,t,u) &= \frac{4}{F_\pi^4}\Big\{(2L_1^r+L_3)(s-2M_\pi^2)^2 + L_2^r[(t-2M_\pi^2)^2 + (u-2M_\pi^2)^2] +\\
&+ (4L_4^r+2L_5^r)M_\pi^2(s-2M_\pi^2) + (8L_6^r+4L_8^r)M_\pi^4\Big\}
\end{aligned}
$$

We have also checked that this amplitude satisfies elastic unitarity.

References

[1] S. Weinberg, *Physica* **96A** (1979) 327.

[2] J. Gasser and H. Leutwyler, *Ann. of Phys.* **158** (1984) 142.

[3] J. Gasser and H. Leutwyler, *Nucl. Phys.* **B250** (1985) 465 and 517.

[4] M.Knetch, B.Moussallam, J.Stern and N.H.Fuchs, *Nucl. Phys.* **B457**(1995) 513.

[5] J.Bijnens, G.Colangelo, G.Ecker, J.Gasser and M.E.Sainio, NORDITA-95/77 N,P; BUTP-95-34;UWThPh-1995-34,HU-TFT-95-64, hep-ph/9511397.

[6] A.M.Bernstein and B.R.Holstein (eds.), Chiral Dynamics: Theory and Experiment, Proceedings of the Workshop held at MIT, Cambridge,MA, USA, July 1994. Springer, Berlin and Heidelberg, 1995.

[7] Tran N. Truong, *Phys. Rev. Lett.* **61** (1988)2526, ibid **D67** (1991) 2260.

[8] A. Dobado, M.J. Herrero and T.N. Truong, *Phys. Lett.* **B235** (1990) 134.

[9] G. Ecker, J. Gasser, A. Pich and E. de Rafael, *Nuc. Phys.* **B321** (1989)311.
G. Ecker, J. Gasser, H. Leutwyler, A. Pich and E. de Rafael, *Phys. Lett.* **B223** (1989)425.
J.F. Donoghue, C. Ramirez and G. Valencia, *Phys. Rev.* **D39**(1989)1947.
V. Bernard, N. Kaiser and U.G. Meißner, *Nuc. Phys.* **B364** (1991)283.

[10] M.Harada, F.Sannino and J.Schechter. SU-4240-642, hep-ph/9511335.

[11] C.J.C. Im, *Phys. Lett.* **B281** (1992) 357;
A. Dobado and J.R. Peláez, *Phys. Lett.* **B286** (1992) 136.
A. Dobado and J.Morales, *Phys. Lett.* **B365** (1996) 264.

[12] A. Dobado and J.R. Peláez, *Phys. Rev.* **D47** (1992) 4883.

[13] T.Hannah, *Phys. Rev.* **D51**(1995) 103, *Phys. Rev.* **D52**(1995)4971.

[14] A.Dobado and J.R.Peláez, *Z. Phys.* **C57**(1993)501.

[15] L.Montanet et al. *Phys. Rev* **D50**, (1994) 1173, and 1995 off-year partial update for the 1996 edition available on the PDG WWW pages (URL:http://pdg.lbl.gov).

[16] J.M. Cornwall, D.N. Levin and G. Tiktopoulos, *Phys. Rev.* **D10** (1974) 1145.
B.W. Lee, C. Quigg and H. Thacker, *Phys. Rev.* **D16** (1977) 1519.
M. Veltman, *Acta Phys. Pol.* **B8** (1977) 475.
M.S. Chanowitz and M.K. Gaillard, *Nucl. Phys.* **B261** (1985) 379.

[17] T. Appelquist and C. Bernard, *Phys. Rev.* **D22** (1980) 200.
A. C. Longhitano, *Nucl. Phys.* **B188** (1981) 118.

[18] A. Dobado and M.J. Herrero, *Phys. Lett.* **B228** (1989) 495 and **B233** (1989) 505.
J. Donoghue and C. Ramirez, Phys. Lett. B234(1990)361. A. Dobado, M.J. Herrero and T.N. Truong, *Phys. Lett.* **B235** (1989) 129.
A. Dobado, M.J. Herrero and J. Terrón, *Z. Phys.* **C50** (1991) 205 and *Z. Phys.* **C50** (1991) 465.
S. Dawson and G. Valencia, *Nucl. Phys.* **B352** (1991)27.
A. Dobado, D. Espriu and M.J. Herrero, *Phys. Lett.* **B255**(1991)405.
D. Espriu and M.J. Herrero,*Nucl. Phys.* **B373** (1992)117.

[19] A.Dobado, M.J.Herrero, J.R.Peláez, E. Ruiz Morales, M.T.Urdiales, *Phys. Lett.* **B352** (1995) 400.
CMS Technical Proposal. CERN/LHC94-38. LHCC/P1.(1994).

[20] A.Dobado and J.R. Peláez, *Nucl. Phys.* **B425**(1994) 110;
Phys.Lett. **B329** (1994) 469. *Addendum*: *Phys.Lett.* **B335** (1994) 554.
H.J. He, Y.P. Kuang and X.Li,*Phys.Lett* **B329** (1994) 278.

[21] V. Bernard, N. Kaiser and U.G. Meißner, *Phys. Rev.* **D43**(1991)2757.

[22] V. Bernard, N. Kaiser and U.G. Meißner, *Nuc. Phys.* **B357** (1991)129.

[23] L.Maiani, G.Pancheri and N.Paver (eds.), *The Second DAΦNE Physics Handbook* (INFN,Frascati,1995).

[24] K.L.Au, D.Morgan and M.R.Pennington, *Phys. Rev.* **D35** (1987)1633.
D. Morgan and Pennington, *Phys. Rev.* **D48** (1993) 1185.

[25] B.S.Zou and D.V.Bugg, *Phys. Rev.* **D48**(1993) 3948.

[26] H.Lehmann, *Phys. Lett.* **B41**(1972)529.

[27] C.Riggenbach, J.F.Donogue, J.Gasser and B.Holstein, *Phys.Rev.* **D43** (1991)127.

[28] J.Bijnens, G.Colangelo, J.Gasser*Nuc. Phys.* **B427** (1994)427.

[29] Protopopescu et al., *Phys.Rev.* **D7** (1973)1279.

[30] Grayer et al., *Nucl. Phys.***B75**(1974)189.

[31] M.J.Losty et al., *Nucl.Phys.***B69**(1974)185.

[32] P.Estabrooks and A.D.Martin, *Nucl.Phys.***B79** (1974)301.

[33] V.Srinivasan et al.,*Phys.Rev* **D12**(1975)681.

[34] L.Rosselet et al.,*Phys.Rev.* **D15**(1977)574.

[35] W.Hoogland et al., *Nucl.Phys* **B126**(1977)109.

[36] R. Mercer et al., *Nucl. Phys.* **B32**(1971) 381.

[37] H.H. Bingham et al., *Nucl. Phys.* **B41** (1972) 1.

[38] D. Linglin et al., *Nucl. Phys.* **B57** (1973) 64.

[39] M.J. Matison et al., *Phys. Rev.* **D9** (1974) 1872.

[40] S.L. Baker et al., *Nucl. Phys.* **B99**(1975) 211.

[41] P. Estabrooks et al., *Nucl. Phys.* **B133**(1978) 490.

[42] J.L. Basdevant, C.D. Froggat and J.L.Petersen, *Nucl. Phys.* **B72**(1974)413.
J.L.Basdevant, P.Chapelle, C.López and M.Sigelle,*Nucl. Phys.* **B98**(1975)285.
C.D.Froggat and J.L. Petersen, *Nucl. Phys.* **B129**(1977)89.
J.L.Petersen, *The $\pi\pi$ interaction.* CERN Yellow report 77-04 (1977).

[43] T.T.Wu and C.N.Yang, *Phys. Rev. Lett.* **13**(1964)380.

[44] J.Gasser and U.-G. Meißner.*Phys. Lett.* **B258**(1991)129.

Recycled Paper

Ernest Orlando Lawrence Berkeley National Laboratory
Technical and Electronic Information Department
University of California | Berkeley, California 94720